# Horizontal Gravity Disturbance Vector in Ocean Dynamics

Peter C. Chu

Department of Oceanography, Naval Postgraduate School, Monterey, CA, USA.

Corresponding author: Peter Chu (pcchu@nps.edu)

**Key Points:**

- Hypothetical Earth gravitation is used in ocean dynamics since the Earth is treated as a point-mass located at the Earth center.
- True Earth gravitation is the volume integration over all the point masses inside the solid Earth.
- Subtraction of hypothetical from true gravitation leads to horizontal gravity disturbance vector which is non-negligible in ocean dynamics.

## Abstract

Oceanographers simplify Newton's law of gravitation, treat the solid Earth as a point-mass located at the Earth's center. This hypothetical simplification is not feasible because the Earth true gravitational force is the volume integration over all point masses inside the solid Earth on a point-mass in oceans. Subtraction of hypothetical gravitation from the true gravitation leads to the gravity disturbance vector $\delta\mathbf{g}$, which is a major variable in geodesy and quantified by gravity field models with observations. On the contrary, $\delta\mathbf{g}$ is totally neglected in oceanography. In this paper, an alternative approach is taken to show the necessity to include $\delta\mathbf{g}$ in ocean dynamics through identifying differences in metric terms and horizontal pressure gradient force among the spherical, spheroidal, and true geopotential coordinates. The horizontal pressure gradient force is the major difference in transformation of true to spheroidal/spherical geopotential coordinates. Such a difference is the horizontal component of $\delta\mathbf{g}$. New hydrostatic balance, geostrophic balance, thermal wind relation, and combined Sverdrup-Stommel-Munk equation are obtained in the spherical geopotential coordinates. Nondimensional (B, D, $F_1$, $F_2$) numbers are used to confirm the importance of gravity disturbance vector versus the traditional forcing terms and calculated from three publicly available datasets. It demonstrates the urgency to include the horizontal gravity disturbance vector in ocean dynamics with commonly used spherical and spheroidal (or related local) geopotential coordinates.



## Plain Language Summary

Newton's law of universal gravitation is for two point-masses or two objects with distance much larger than their sizes. The true Earth gravitational force is the volume integration over all point masses inside the solid Earth on a point-mass in oceans. However, oceanographers treat the solid Earth as a point-mass with the whole Earth mass located at the Earth's center. The gravitational force of the solid Earth becomes the force between the hypothetical point-mass on the Earth center and the point-mass in oceans. Subtraction of hypothetical gravitation from the true gravitation leads to the gravity disturbance vector. Three publicly available datasets in climatological, geodetic, and oceanographic communities are used to confirm the importance of the horizontal gravity disturbance vector in ocean dynamics.


## 1 Introduction

Newton's law of universal gravitation in today's language states that every point mass attracts every other point mass by a force acting along the line intersecting the two points. The force is proportional to the product of the two masses, and inversely proportional to the square of the distance between them. The gravitational force ($\mathbf{F}_N$) of solid Earth on a point mass ($m_A$) at location $\mathbf{r}_A$ in atmosphere and oceans is the volume integration over all the point masses located at $\mathbf{r}$ inside the solid Earth on $m_A$ in oceans (Figure 1) with the formula [Equation (6.4) in Vaníček and Krakiwsky 1986]

$$\mathbf{F}_N(\mathbf{r}_A) = m_A\mathbf{n},\ \ \mathbf{n} = Gm_A\iiint_{\Pi}\frac{\sigma(\mathbf{r})}{|\mathbf{r}-\mathbf{r}_A|^3}(\mathbf{r}-\mathbf{r}_A)d\Pi \tag{1}$$

where $G = 6.67408\times10^{-11}\mathrm{Nm^2kg^{-2}}$, is the Newtonian gravitational constant; $[\sigma(\mathbf{r}), \Pi]$ are the mass density and volume of the solid Earth; $\mathbf{n}$ is the *true* gravitational acceleration, and the

Earth center is the origin of the position vectors $\mathbf{r}$ and $\mathbf{r}_A$. Let $\sigma_0$ be the average mass density. With $\sigma_0$, Eq (1) becomes,

$$\mathbf{F}_N(\mathbf{r}_A) = -m_A \frac{GM}{|\mathbf{r}_A|^3}\mathbf{r}_A + Gm_A \iiint_{\Pi} \frac{[\sigma(\mathbf{r}) - \sigma_0]}{|\mathbf{r} - \mathbf{r}_A|^3}(\mathbf{r} - \mathbf{r}_A)d\Pi \quad (2)$$

where $M = \sigma_0\Pi = 5.98\times10^{24}$ kg is the total mass of the solid Earth.

Every oceanographer including the author from very beginning of the career learned that the Earth gravity on the point mass ($m_A$) in oceans at location $\mathbf{r}_A$ consists of "gravitational force" and centrifugal force (Figure 2). However, the solid Earth is treated as a point mass located at the Earth center **O** with the total Earth mass. With such a simplified treatment, a hypothetical "gravitational force" of the solid Earth on the point mass ($m_A$) in oceans is not $\mathbf{F}_N(\mathbf{r}_A)$ represented by (2) but $\mathbf{F}_0(\mathbf{r}_A)$ given by

$$\mathbf{F}_0(\mathbf{r}_A) = -m_A\mathbf{n}_0, \quad \mathbf{n}_0 = \frac{GM}{|\mathbf{r}_A|^3}\mathbf{r}_A \quad (3)$$

where $\mathbf{n}_0$ is the hypothetical gravitational acceleration.

Let $\boldsymbol{\Omega}$ be the Earth's angular velocity with $|\boldsymbol{\Omega}| = 2\pi/(86164\text{ s})$. Combination of the true gravitational acceleration $\mathbf{n}$ and the centrifugal acceleration $\mathbf{a}_c$ leads to the true gravity $\mathbf{g}_t$,

$$\mathbf{g}_t = \mathbf{n} + \mathbf{a}_c, \quad \mathbf{a}_c = \boldsymbol{\Omega}\times(\boldsymbol{\Omega}\times\mathbf{r}_A) \quad (4)$$

Combination of the hypothetical gravitational acceleration $\mathbf{n}_0$ and the centrifugal acceleration $\mathbf{a}_c$ leads to the effective gravity (sometimes called normal gravity, or apparent gravity),

$$\mathbf{g}_e = \mathbf{n}_0 + \mathbf{a}_c, \quad \mathbf{a}_c = \boldsymbol{\Omega}\times(\boldsymbol{\Omega}\times\mathbf{r}_A) \quad (5)$$

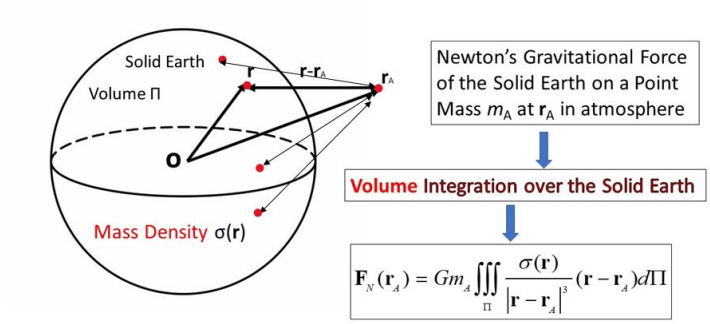


**Figure 1**. Newtonian gravitational attraction of a point mass located at **r** inside the solid Earth on a point mass located at $\mathbf{r}_A$ in atmosphere. The gravitational force of the solid Earth on a point mass $m_A$ at $\mathbf{r}_A$ is the volume integration, and non-radial [i.e., $\mathbf{F}_N(\mathbf{r}_A)$ is not pointing to the center **O**] [after Chu (2023)].

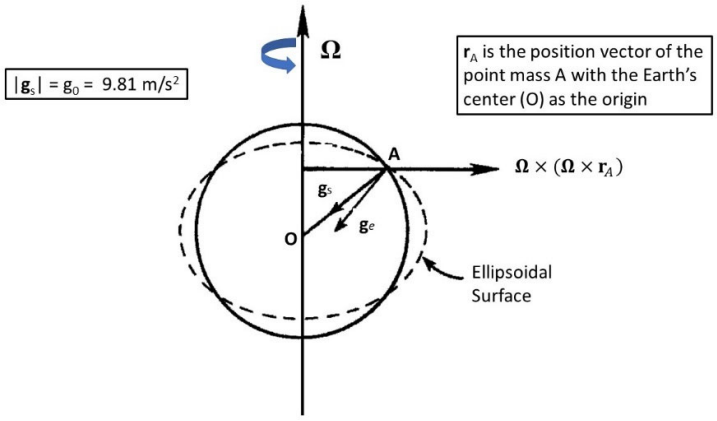


**Figure 2.** The solid Earth is treated as a point mass located at the Earth center (**O**) with the whole Earth mass. It is called in oceanography as the "gravitational force" of the solid Earth on the point mass A in the oceans. The associated standard gravity $\mathbf{g}_s$ is radial (pointing to the center **O**). The combination of hypothetical "gravitational acceleration" and the centrifugal acceleration leads to the effective gravity $\mathbf{g}_e$, which is non-radial [after Chu (2023)].

Subtraction of the hypothetical gravitational acceleration ($\mathbf{n}_0$) from the true gravitational acceleration ($\mathbf{n}$) leads to the gravity disturbance vector ($\delta\mathbf{g}$),

$$\delta\mathbf{g} \equiv \mathbf{n} - \mathbf{n}_0 = G\iiint_{\Pi} \frac{[\sigma(\mathbf{r}) - \sigma_0]}{|\mathbf{r} - \mathbf{r}_A|^3}(\mathbf{r} - \mathbf{r}_A)d\Pi = \mathbf{g}_t - \mathbf{g}_e \tag{6}$$

where Eqs (1), (3)-(5) are used. Obviously, the gravity disturbance vector $\delta\mathbf{g}$ is neglected completely in oceanography although it is a major variable in geodesy.

The gravity disturbance vector $\delta\mathbf{g}$ due to the nonuniform mass density $\sigma(\mathbf{r})$ inside the solid Earth [see Eq (6)] is represented by the disturbing gravity potential $T$. The true geopotential and true gravity in oceans are given by (Sandwell and Smith 1997; Kostelecký et al. 2015; Chu 2023)

$$\Phi_t \equiv \Phi_e - T(\lambda, \varphi, z), \quad T(\lambda, \varphi, z) \approx g_0 N(\lambda, \varphi), \quad g_0 = 9.81 \text{m s}^{-2} \tag{7}$$

where ($\Phi_t$, $\Phi_e$) are (true, spheroidal) geopotentials; $N$ is the geoidal undulation; and $g_0$ is the reference gravity. The second approximated formula in (7) is obtained from the thin ocean depth in comparison to the Earth radius. The true gravity $\mathbf{g}_t$, effective gravity $\mathbf{g}_e$, and gravity disturbance vector $\delta\mathbf{g}$ are represented by,

$$\mathbf{g}_t = -\nabla_3\Phi_t, \quad \mathbf{g}_e = -\nabla_3\Phi_e, \quad \delta\mathbf{g} \approx g_0\nabla N \tag{8}$$

where $\nabla_3$ is the three-dimensional vector differential operator; and $\nabla$ is the horizontal vector differential operator.

The ultimate cause of using gravity rather than using gravitational acceleration in meteorology and oceanography is to *make the centrifugal acceleration* $\mathbf{a}_c$ *vanish* in the equation of motion. Thus, two basic rules are always followed by meteorologists and oceanographers consciously or unconsciously:

**Rule - 1.** The centrifugal acceleration $\mathbf{a}_c$ should never occur in the atmospheric and oceanic dynamics such as in the equation of motion.

**Rule - 2.** The gravity should never be split into gravitational accelerationand centrifugal acceleration $\mathbf{a}_c$.

Breaking these two rules is equivalent to destroying the foundation of the atmospheric and oceanic dynamics. All the efforts that meteorologists and oceanographers have made will vanish.

Chu (2021a, b, c) introduce $\mathbf{g}_t$ into the atmospheric and oceanic dynamics, i.e., include the gravity disturbance vector $\delta\mathbf{g}$ (then called horizontal gravity $\mathbf{g}_h$) in the basic equations of motion. Chang and Wolfe (2022) (https://www.nature.com/articles/s41598-022-09967-3) (hereafter referred CW22) and Stewart and McWilliams (2022) (see website: https://www.nature.com/articles/s41598-022-10023-3.) (hereafter referred to SM22) challenged Chu's work. CW22's and SM22's comments to Chu (2021a, b, c) with obvious and severe errors (see Appendix A) were published in the Scientific Reports (SR). However, Chu's replies to CW22's and SM22's comments submitted to SR (also sent to the four authors of CW22 and SM22 on 20 April 2022) was rejected and the paper (Chu, 2021a) was mistakenly retracted by the Chief Editor of SR. Several months later, then Editor-in-Chief of the Journal of Geophysical Research – Atmospheres (Dr. Minghua Zhang) disregarded Chu 's responses and retract the paper (Chu 2021b) on 30 September 2022 with the wrong statement (https://agupubs.onlinelibrary.wiley.com/doi/10.1002/jgrd.58211).

Recently, Chu (2023) demonstrated the importance of the horizontal gravity disturbance vector in atmospheric dynamics (see website: https://www.sciencedirect.com/science/article/pii/S0377026523000209.) Chang et al. (2023) commented on Chu (2023) (hereafter referred CWSM23) to the Dynamics of Atmospheres and Oceans (DAO) with the same mistakes (https://www.sciencedirect.com/science/article/pii/S0377026523000337).

The three completely wrong comments (CW22, SM22, CWMS23) have misled and continue to mislead the oceanographic and meteorological communities. To eliminate the negative influences by CW22, SM22, and CWMS23, an alternative approach (easily accepted by the oceanographic and meteorological communities) is taken here using the spheroidal, spherical, and true geopotential coordinates (Section 2), transforming from the true to spheroidal/spherical geopotential coordinates (Section 3), and representing the sea level in the true and spheroidal geopotential coordinates (Section 4). Three publicly available datasets from geodetic and oceanographic communities are used to effectively identify the importance of the horizontal gravity disturbance vector $g_0\nabla N$ in ocean dynamics (Section 5). Basic dynamic equations with the true geopotential in the spherical geopotential coordinates are presented (Section 6). New equations for the geostrophic current and thermal wind relation (Section 7), 1½ layer model with rigid lid (Section 8), and the combined

Sverdrup-Stommel-Munk dynamics (Section 9) are derived. Importance of the horizontal gravity disturbance vector is identified using these new equations and the open-source datasets described in Section 5. New spheroidal and spherical geopotential approximations are proposed for the transformation from true to spheroidal/spherical geopotential coordinates (Section 10). With such new approximations, the horizontal gravity disturbance vector $g_0\nabla N$ should be added to the existing horizontal momentum equation. Section 11 presents the conclusions. Appendix A lists major mistakes in CW22, SM22, CWSM23, and additional comments of Dr. Chang on Chu (2021 a, b, c, 2023) submitted to DAO (presented in Appendix B).

## 2. Spheroidal, Spherical, and True Geopotential Coordinates

Geopotential surface is a surface of constant geopotential with gravity perpendicular to it. The geopotential surface is solely determined by gravity. Associated with three types of gravity, effective gravity ($\mathbf{g}_e$), standard gravity ($\mathbf{g}_s$), and true gravity ($\mathbf{g}_t$), we have spheroidal, spherical, and true geopotentials, with corresponding geopotential surfaces.

The concentric oblate spheroidal geopotential ($\Phi_e$) surfaces are corresponding to the effective gravity (or sometimes called apparent gravity) $\mathbf{g}_e$,

$$\mathbf{g}_e = -g_0\mathbf{k}_e, \tag{9}$$

where $\mathbf{k}_e$ is the unit vector perpendicular to the spheroidal surfaces (Figure 3). The centrifugal acceleration $\mathbf{a}_c$ is also in the direction of $\mathbf{k}_e$. The effective gravity ($\mathbf{g}_e$) uses uniform Earth mass density [see Eqs (3), (5)]. Such concentric oblate spheroidal surfaces are the *spheroidal geopotential surfaces*. The corresponding horizontal equation of motion without friction is given by,

$$\left(\frac{D\mathbf{U}_e}{Dt}\right)_e + 2\boldsymbol{\Omega}\times\mathbf{U}_e = -\left(\frac{1}{\rho}\nabla p\right)_e + \mathbf{F} \tag{10}$$

where $\rho$ is the density; $p$ is pressure; $\mathbf{U}$ is the horizontal velocity vector; $\mathbf{F}$ is the frictional force; and the subscript '$e$' means for the effective gravity.

The concentric spherical geopotential ($\Phi_s$) surfaces are corresponding to the standard gravity,

$$\mathbf{g}_s = -g_0\mathbf{k}_s \tag{11}$$

where $\mathbf{k}_s$ is the unit vector perpendicular to the spherical surfaces (Figure 4a), i.e., in the direction of the position vector $\mathbf{r}$ relative to the Earth center $\mathbf{O}$. Such spherical surfaces are *spherical geopotential surfaces*. The spherical geopotential uses uniform Earth mass density, and subjectively eliminates the meridional component of the centrifugal acceleration (Figure 4b). Figure 4c shows the difference between the difference between $\mathbf{k}_s$ and $\mathbf{k}_e$. The

184 corresponding horizontal equation of motion without friction for the standard gravity $\mathbf{g}_s$ is
185 given by,

186 $$\left(\frac{D\mathbf{U}_s}{Dt}\right)_s + 2\boldsymbol{\Omega}\times\mathbf{U}_s = -\left(\frac{1}{\rho}\nabla p\right)_s + \mathbf{F} \qquad (12)$$

187 where the subscript '*s*' means for the standard gravity.
188

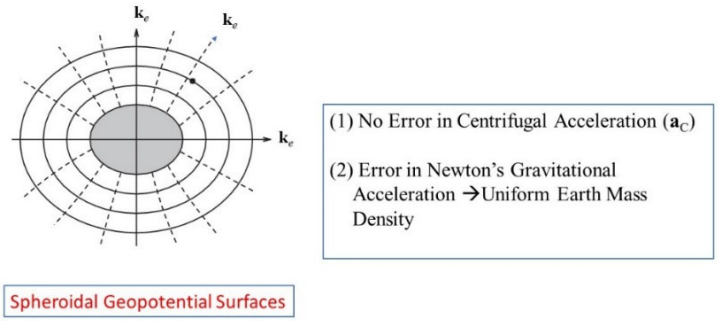


189

190 **Figure 3**. Spheroidal geopotential surfaces and unit vector $\mathbf{k}_e$ corresponding to the effective
191 gravity ($\mathbf{g}_e$).
192

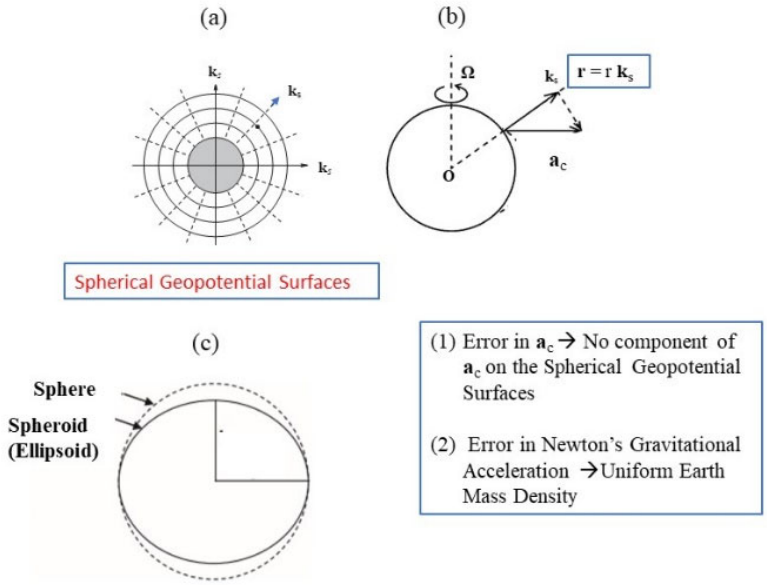


193

194 **Figure 4**. Spherical geopotential corresponding to the standard gravity $\mathbf{g}_s$: (a) spherical
195 geopotential surfaces, (b) error in centrifugal acceleration, and (c) comparison between
196 spherical and spheroidal geopotential surfaces.

197

198 The true geopotential ($\Phi_t$) surfaces are corresponding to the true gravity $\mathbf{g}_t$,

199 $$\mathbf{g}_t = -g_0 \mathbf{k}_t \tag{13}$$

200 where $\mathbf{k}_t$ is the unit vector perpendicular to the true-geopotential surfaces, with the geoid
201 being one of them (Figure 5). The angle between $\mathbf{k}_t$ and $\mathbf{k}_e$ is the deflection of vertical
202 (Figure 6). The horizontal (on the true geopotential surfaces such as geoid surface) equation
203 of motion without friction is given by,

204 $$\left(\frac{D\mathbf{U}_t}{Dt}\right)_t + 2\boldsymbol{\Omega} \times \mathbf{U}_t = -\left(\frac{1}{\rho}\nabla p\right)_t + \mathbf{F} \tag{14}$$

205 where the subscript '*t*' means for the true gravity (on the true geopotential surfaces). The
206 geoid is the one true geopotential ($\Phi_t$) surface corresponding to the true gravity $\mathbf{g}_t$ with
207 horizontal variation from 85 m to -106 m (http://icgem.gfz-potsdam.de/home).

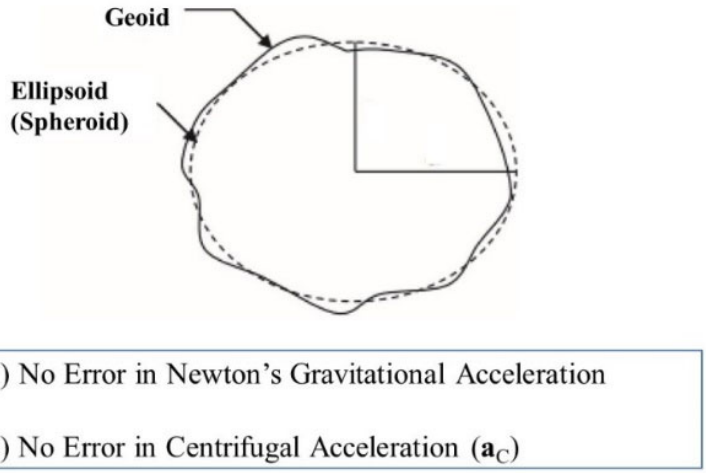


208

209 **Figure 5**. Illustration of spheroidal surface and geoid about the spheroidal surface. The true
210 geopotential surface is the geoidal surface.

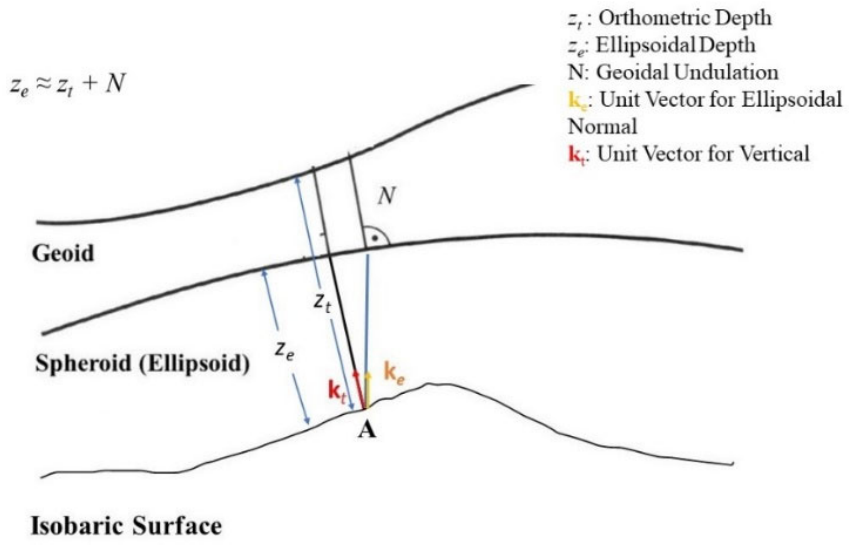


211

212 **Figure 6**. Orthometric depth ($z_t$), spheroidal depth ($z_e$), geoidal undulation ($N$), and deflection
213 of vertical (i.e., angle between $\mathbf{k}_t$ and $\mathbf{k}_e$). Note that $z_e \le 0$.

214

215 **3. Transformation from the True to Spheroidal/Spherical Geopotential Coordinates**

216 Subtraction of (10) from (14) leads to the difference between using the true and
217 spheroidal geopotential coordinates,

218 $$2\boldsymbol{\Omega}\times(\mathbf{U}_t-\mathbf{U}_e)=\varepsilon^{(m)}_{t\to e}+\varepsilon^{(p)}_{t\to e},\quad \varepsilon^{(m)}_{t\to e}\equiv\left[\left(\frac{D\mathbf{U}_e}{Dt}\right)_e-\left(\frac{D\mathbf{U}_t}{Dt}\right)_t\right],\varepsilon^{(p)}_{t\to e}\equiv\left[\frac{1}{\rho}(\nabla p)_e-\frac{1}{\rho}(\nabla p)_t\right] \quad (15)$$

219 where $\varepsilon^{(m)}_{t\to e}$ is the difference in metric terms (Gill 1982); and $\varepsilon^{(p)}_{t\to e}$ is the difference in
220 horizontal pressure gradient. The subscript "$t\to e$" represents the replacement of true
221 geopotential by spheroidal geopotential coordinates. Both differences represent the missing
222 terms in the spheroidal geopotential coordinates using the true gravity $\mathbf{g}_t$.
223 From Figure 6, the location of point-mass A can be determined by ($\lambda$, $\varphi$, $z_e$) in the
224 spheroidal geopotential coordinates and ($\lambda$, $\varphi$, $z_t$) in the true geopotential coordinates with
225 irregular geometry (not yet established and just for illustration). Here, $z_e$ ($\le 0$) is the
226 spheroidal (ellipsoidal) depth; $z_t$ ($\le -N$) is the geoidal depth; ($\lambda$, $\varphi$) are longitude and latitude.
227 The spheroidal geopotential surfaces are represented by,

228 $$z_e = \text{const} \quad (16)$$

229 The true geopotential surfaces are represented by,

230 $$z_t = \text{ const} \quad (17)$$

231 with

232 $$z_t = z_e - N(\lambda,\varphi) \quad (18)$$

where the geoid undulation ($N$) varies from -106.2 m to 85.83 m (Figure 7) from the EIGEN6C4 gravity model (Kostelecký et al., 2015).

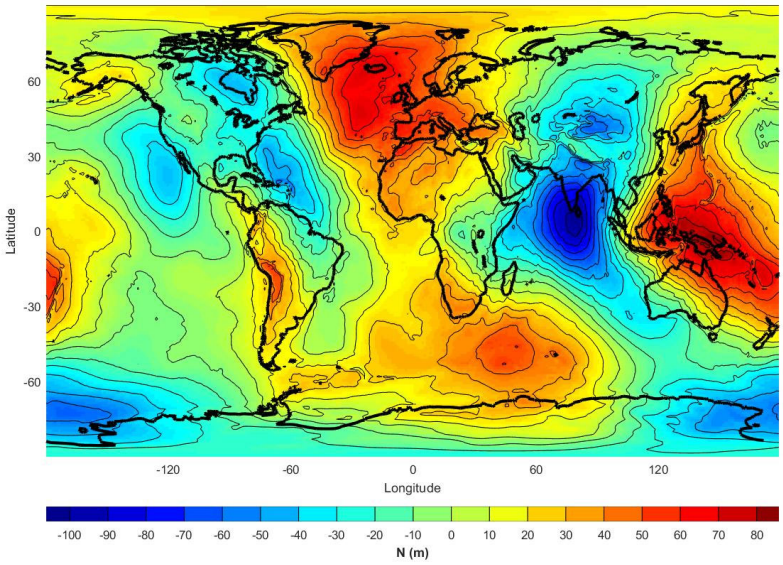


**Figure 7.** Digital data for EIGEN-6C4 geoid undulation ($N$) with 1°×1°, computed online at the website http://icgem.gfz-potsdam.de/home.

In the true geopotential coordinate ($\lambda$, $\varphi$, $z_t$), the true gravity $\mathbf{g}_t$ does not have component on the true geopotential surfaces (i.e., the true horizontal surfaces). The hydrostatic balance equation with the true gravity $\mathbf{g}_t$ is given by,

$$\frac{\partial p}{\partial z_t} = -\rho g_0 \tag{19}$$

A derivative with respect to $\lambda$ between the $z_e$ and $z_t$ as the vertical coordinates is given by,

$$\left(\frac{\partial}{\partial \lambda}\right)_{z_e} = \left(\frac{\partial}{\partial \lambda}\right)_{z_t} + \left(\frac{\partial z_t}{\partial \lambda}\right)_{z_e} \frac{\partial}{\partial z_t} \tag{20}$$

Using (20) to the derivative of $p$ gives

$$\left(\frac{\partial p}{\partial \lambda}\right)_{z_e} = \left(\frac{\partial p}{\partial \lambda}\right)_{z_t} + \left(\frac{\partial z_t}{\partial \lambda}\right)_{z_e} \frac{\partial p}{\partial z_t} \tag{21}$$

Substitution of (18) and (19) into (21) leads to

$$\left(\frac{\partial p}{\partial \lambda}\right)_{z_e} = \left(\frac{\partial p}{\partial \lambda}\right)_{z_t} + \rho g_0 \frac{\partial N}{\partial \lambda} \tag{22}$$

We obtain the following relationship after conducting similar operation for $\varphi$,

$$(\nabla p)_t = (\nabla p)_e - \rho g_0 \nabla_e N \tag{23}$$

Substitution of (23) into the last equation in (15) leads to

$$\boxed{\varepsilon^{(p)}_{t\to e} = \left[\frac{1}{\rho}(\nabla p)_e - \frac{1}{\rho}(\nabla p)_t\right] = g_0 \nabla_e N} \tag{24}$$

which shows that *the difference in horizontal pressure gradient force between the true and spheroidal geopotential coordinates is the horizontal gravity disturbance vector* ($g_0\nabla N$). Substitution of (24) into (15) gives,

$$2\boldsymbol{\Omega}\times(\mathbf{U}_t - \mathbf{U}_e) = \varepsilon^{(m)}_{t\to e} + g_0\nabla_e N \tag{25}$$

Substitution of (15) and (25) into (14) leads to

$$\left(\frac{D\mathbf{U}_t}{Dt}\right)_e + 2\boldsymbol{\Omega}\times\mathbf{U}_t = \varepsilon^{(m)}_{t\to e} - \left(\frac{1}{\rho}\nabla p\right)_e + g_0\nabla_e N + \mathbf{F} \tag{26}$$

Here, the first term of the righthand side is the metric term error. Meteorological and oceanographic communities have the consensus that the metric term error is negligible (e.g., Gill 1982, CW22, CWSM23),

$$\varepsilon^{(m)}_{t\to e} \approx 0 \tag{27}$$

Eq (26) is simplified into,

$$\left(\frac{D\mathbf{U}_t}{Dt}\right)_e + 2\boldsymbol{\Omega}\times\mathbf{U}_t = -\left(\frac{1}{\rho}\nabla p\right)_e + g_0\nabla_e N + \mathbf{F} \tag{28}$$

which is the horizontal equation of motion in the spheroidal geopotential coordinates using the true geopotential (i.e., true gravity $\mathbf{g}_t$).

Subtraction of (12) from (10) leads to the difference between using the spherical and spheroidal geopotential coordinates,

$$2\boldsymbol{\Omega}\times(\mathbf{U}_e - \mathbf{U}_s) = \varepsilon^{(m)}_{e\to s} + \varepsilon^{(p)}_{e\to s},$$
$$\varepsilon^{(m)}_{e\to s} \equiv \left[\left(\frac{D\mathbf{U}_s}{Dt}\right)_s - \left(\frac{D\mathbf{U}_e}{Dt}\right)_e\right],\ \varepsilon^{(p)}_{e\to s} \equiv \left[\frac{1}{\rho}(\nabla p)_s - \frac{1}{\rho}(\nabla p)_e\right] \tag{29}$$

where $\varepsilon^{(m)}_{e\to s}$ is the difference in metric terms; and $\varepsilon^{(p)}_{e\to s}$ is the difference in horizontal pressure gradient force. The subscript "$e\to s$" represents the replacement of spheroidal by spherical geopotential coordinates. Both differences represent the missing terms in the spherical geopotential coordinates using the spheroidal geopotential (i.e., effective gravity $\mathbf{g}_e$). Estimation of error due to such replacement has been conducted through analytical analysis and numerical solutions of equations in spheroidal and spherical coordinates. The analytical analysis was conducted only for the difference in metric terms $\varepsilon^{(m)}_{e\to s}$ which is less than 0.17% (Gill 1982). More recently, solutions of the spheroidal (spheroidal geopotential coordinates) and spherical (spherical geopotential coordinates) equations were obtained. The differences

in metric terms and horizontal pressure gradient force between the solutions are likely to be small,

$$\varepsilon_{e\to s}^{(m)} + \varepsilon_{e\to s}^{(p)} \approx 0 \tag{30}$$

except perhaps in long-term simulations in which small systematic differences may accumulate (Gates 2004, Beńard 2015, Staniforth and White 2015). These studies are very useful because nearly all the analytical and numerical atmospheric and oceanic models use spherical coordinates (or local coordinates related to the spherical coordinates).

The difference between using the true and spherical geopotential coordinates can be estimated by

$$2\boldsymbol{\Omega}\times(\mathbf{U}_t - \mathbf{U}_s) = 2\boldsymbol{\Omega}\times(\mathbf{U}_t - \mathbf{U}_e) + 2\boldsymbol{\Omega}\times(\mathbf{U}_e - \mathbf{U}_s) \tag{31}$$

Substitution of (25) and (29) into (31) leads to

$$2\boldsymbol{\Omega}\times(\mathbf{U}_t - \mathbf{U}_s) = \varepsilon_{t\to e}^{(m)} + g_0\nabla_e N + \varepsilon_{e\to s}^{(m)} + \varepsilon_{e\to s}^{(p)} \tag{32}$$

Substitution of (32) into (14) leads to

$$\left(\frac{D\mathbf{U}_t}{Dt}\right)_s + 2\boldsymbol{\Omega}\times\mathbf{U}_t = -\left(\frac{1}{\rho}\nabla p\right)_s + g_0\nabla_s N + \mathbf{F} \tag{33}$$

where Eq (27) and Eq (30) are used. Eq (33) is the horizontal equation of motion in the spherical geopotential coordinates using the true geopotential (i.e., true gravity $\mathbf{g}_t$.)

## 4. Representation of Sea Level in True and Spheroidal Geopotential Coordinates

Different from the three geopotential surfaces which are solely determined by gravity, the sea level is a physical surface and can be represented by various coordinate systems with different values noted as the sea surface height. In oceanography and meteorology, the sea surface height is always referenced to the spheroidal geopotential coordinates ($h_e$) such as in measurement by satellite altimetry https://ggos.org/item/satellite-altimetry/. However, the sea level can also be represented in the true geopotential coordinates ($h_t$), $z_t = z_e - N$ [see Eq (18)]. Table 1 shows different representations of sea surface height, mean sea level (MSL), and global MSL in spheroidal and true geopotential coordinates. The MSL is *under the influence of other forces such as winds, tides, currents, and Coriolis force in addition to gravity*. Thus, the MSL is not a geopotential surface of any type.

No matter using, $h_e$ or $h_t$, MSL is the SAME surface. The mean sea level pressure (MSLP) is evaluated at MSL no matter using the spheroidal or true geopotential coordinates. This is to say that the MSLP is independent of the coordinate systems and always computed at MSL, and not at the geoid and the ellipsoid. MSLP is evaluated or computed on $z_e = S(\lambda, \varphi)$ in the spheroidal geopotential coordinates, and on $z_t = S(\lambda, \varphi) - N(\lambda, \varphi)$ in the true-geopotential coordinates. MSLP is NEVER evaluated on the ellipsoidal or geoidal surface.

**Table 1.** Representation of sea surface height, MSL, global MSL in the spheroidal and true geopotential coordinate systems.

| | Spheroidal Geopotential Coordinates $(\lambda, \varphi, z_e)$ | True Geopotential Coordinates $(\lambda, \varphi, z_t)$ | Transforming True to Spheroidal Geopotential Coordinates |
|---|---|---|---|
| Geopotential Surface with Best Fitting to the Global MSL | Earth Reference Ellipsoidal Surface | Geoid Surface | |
| Sea Surface Height | $z_e = h(\lambda, \varphi, t)$ | $z_t = h(\lambda, \varphi, t)$ $-N(\lambda, \varphi)$ | $z_t = z_e - N(\lambda, \varphi)$ |
| MSL: $S(\lambda,\varphi) = \langle h(\lambda,\varphi,t)\rangle_{\text{Temporal Average}}$ | $z_e = S(\lambda, \varphi)$ | $z_t = S(\lambda, \varphi)$ $-N(\lambda, \varphi)$ | |
| Global MSL: $S^* = [S(\lambda,\varphi)]_{\text{Spatial Average}}$ =const | $z_e = 0$ | $z_t = -N(\lambda,\varphi)$ | |
| Horizontal Pressure Gradient | | | $(\nabla p)_t = (\nabla p)_e - \rho g_0 \nabla_e N$ |

## 5. Data Sources

Three publicly available datasets are used to effectively identify the importance of the horizontal gravity disturbance vector $g_0 \nabla N$ in ocean dynamics: (a) the global static gravity field model EIGEN-6C4 for the geoid $N$ (from http://icgem.gfz-potsdam.de/home,) (b) the climatological annual mean temperature and salinity from the NCEI WOA18 (Boyer et al., 2018) for the sea water density ($\rho$) data (from https://www.ncei.noaa.gov/access/world-ocean-atlas-2018/,) and (c) the climatological annual mean surface wind stress ($\tau_\lambda$, $\tau_\varphi$) from the Atlas of Surface Marine Data 1994 (SMD94) (from https://iridl.ldeo.columbia.edu/SOURCES/.DASILVA/.) The geoid ($N$) data are represented in the spherical geopotential coordinate system since the gravity disturbance vector $\delta\mathbf{g}$ is independent on the Earth rotation [see Eq (6)]. However, the oceanographic data WOA18 and the climatological data SMD94 are represented in the effective geopotential coordinate system (i.e., the oblate spheroidal coordinates) with $z = 0$ as the surface. In this study, all the computation is in the spherical geopotential coordinates.

The difference between the spherical and spheroidal geopotential coordinate systems are estimated less than 0.17% (Gill 1982), and likely to be small except perhaps in long-term simulations in which small systematic differences may accumulate (Gates 2004, Beńard 2015). In this study, all the computation is in the spherical geopotential coordinates.

## 6. Basic Dynamic Equations with True Geopotential in Spherical Geopotential Coordinates

Large-scale ocean circulation under Boussinesq approximation in the spherical geopotential (or related local) coordinates using the true gravity is governed by the momentum equation, i.e., from Eq (33) (hereafter the subscript 's' and '$t$' are removed for simplicity),

$$\rho_0\left[\frac{D\mathbf{U}}{Dt}+f\mathbf{k}\times\mathbf{U}\right]=-\nabla p+\rho g_0\nabla N+\rho_0(\mathbf{F}_h+\mathbf{F}_v) \tag{34}$$

and the continuity equation

$$\nabla\bullet\mathbf{U}+\frac{\partial w}{\partial z}=0 \tag{35}$$

where $w$ is the vertical velocity; $\rho_0$ = 1,028 kg m$^{-3}$, is the reference density; $f = 2\Omega \sin\varphi$, is the reference Coriolis parameter; ($\mathbf{F}_h$, $\mathbf{F}_v$) are the frictional forces which are parameterized by horizontal and vertical shears,

$$\mathbf{F}_h = A\nabla^2\mathbf{U},\quad \mathbf{F}_v=\frac{\partial}{\partial z}\left(K\frac{\partial\mathbf{U}}{\partial z}\right) \tag{36}$$

where ($A$, $K$) are the corresponding eddy viscosities. The turbulent momentum flux is given by

$$\rho_0 K\frac{\partial\mathbf{U}}{\partial z}|_{z=0}=\boldsymbol{\tau} \tag{37}$$

at the rigid-lid ocean surface ($z$ = 0) with $\boldsymbol{\tau}$ the wind stress; and is given by

$$K\frac{\partial\mathbf{U}}{\partial z}|_{z=-H}=\gamma\mathbf{M},\quad \mathbf{M}\equiv\int_{-H}^{0}\mathbf{U}dz \tag{38}$$

at the lower boundary (z = -$H$). Here, $\mathbf{M}$ is the volume transport; γ is the Rayleigh friction coefficient (Stommel 1948). When γ = 0, Eq (38) shows negligible turbulent momentum flux at $z$ = -$H$ (Sverdrup 1947, Munk 1950).

With the constant reference density $\rho_0$, the three-dimensional hydrostatic equilibrium between the pressure gradient force and the true gravity $\mathbf{g}_t$[= $-\nabla_3\Phi_t$, $\Phi_t = g_0(z - N)$] is given by

$$-\nabla_3 p_0-\rho_0\nabla_3\Phi=0 \tag{39}$$

where

$$p_0=-\rho_0 g_0(z-N) \tag{40}$$

is the reference pressure corresponding to the reference density $\rho_0$. Subtraction of (39) from (34) leads to

$$\boxed{\rho_0\left[\frac{D\mathbf{U}}{Dt}+f\mathbf{k}\times\mathbf{U}\right]=-\nabla\hat{p}+(\rho-\rho_0)g_0\nabla N+\rho_0(\mathbf{F}_h+\mathbf{F}_v)} \tag{41}$$

$$\frac{\partial\hat{p}}{\partial z}=-(\rho-\rho_0)g_0 \tag{42}$$

where $\hat{p} = p - p_0$, is the dynamic pressure; and Eq (42) is the hydrostatic balance in the vertical direction.

## 7. Geostrophic current and thermal wind relation

For steady-state low Rossby number flow (negligible nonlinear advection) without friction, i.e., $D\mathbf{U}/Dt = 0$, and $\mathbf{F}_h = 0$, $\mathbf{F}_v = 0$ in Eq (41), we have

$$\boxed{f\mathbf{k}\times\mathbf{U} = -\frac{1}{\rho_0}\nabla\hat{p} + \frac{\rho-\rho_0}{\rho_0}g_0\nabla N} \tag{43}$$

which is a new geostrophic balance with an extra term due to the horizontal gravity disturbance vector ($g_0\nabla N$). The thermal wind relation can be derived from (42) and (43)

$$\boxed{f\frac{\partial\mathbf{U}}{\partial z} = \mathbf{k}\times\left[-(g_0/\rho_0)\nabla\rho + \Theta^2\nabla N\right],\quad \Theta^2 \equiv -\left(\frac{g_0}{\rho_0}\frac{\partial\rho}{\partial z}\right)} \tag{44}$$

where $\Theta$ is the buoyancy frequency. A depth-dependent non-dimensional $D$ number is defined,

$$D(z) = \frac{O\left(\left|\Theta^2\nabla N\right|\right)}{O\left(\left|(g_0/\rho_0)\nabla\rho\right|\right)} \approx \frac{\text{mean}\left(\left|\Theta^2\nabla N\right|\right)}{\text{mean}\left(\left|(g_0/\rho_0)\nabla\rho\right|\right)} \tag{45}$$

to identify the importance of the horizontal gravity disturbance vector versus the horizontal density gradient (baroclinicity). Hereafter, the mean values are used to represent the orders of magnitude.

The WOA18 annual mean temperature and salinity data are used to compute $\rho$ and $\Theta^2$. The static gravity data EIGEN-6C4 is used to get $N$. With given ($\rho$, $\Theta^2$, $N$), two vectors $(g_0/\rho_0)\nabla\rho$ and $\Theta^2\nabla N$ are computed at all grid ($1^o\times1^o$) points and $z$-levels (z = 0 to -5,500 m) of the WOA18. Figures 8 and 9 show the contour plots and Figures 10 and 11 show the histograms of $|(g_0/\rho_0)\nabla\rho|$ and $|\Theta^2\nabla N|$ for the four levels, z = 0, -500, -1,000, -2,000 m. The magnitude $|(g_0/\rho_0)\nabla\rho|$ has the mean of 13.45 Eotvos (1 Eotvos = $10^{-9}s^{-2}$) at z = 0, 2.154 Eotvos at z = -500 m, 1.245 Eotvos at z = -1,000 m, and 0.5615 Eotvos at z = - 2,000 m (Figure 10). The magnitude $|\Theta^2\nabla N|$ has mean of 1.128 Eotvos at $z$ = 0, 0.4789 Eotvos at $z$ = -500 m, 0.4389 Eotvos at $z$ = -1,000 m, and 0.3894 Eotvos at $z$ = -2,000 m (Figure 11). The $D$ number (Figure 12) increases with depth almost monotonically from 8.4% at z = 0, 22.2% at z = -500 m, 35.3% at z = -1,000 m, 69.3% at z = -2,000 m, 81.4% at z = -3,000 m, 108.7% at z = -4,000 m, and 157.6% at z = -5,000 m. These D numbers demonstrate the importance of the horizontal gravity disturbance vector in the geostrophic current and thermal wind relation.

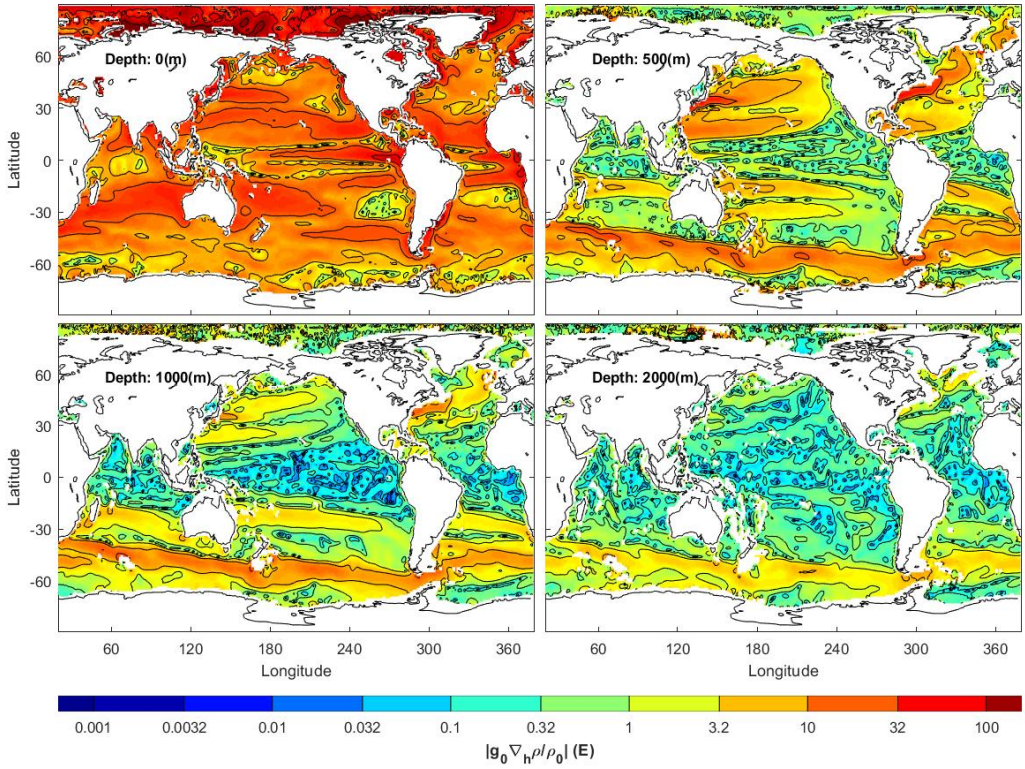


**Figure 8.** Horizontal contour plots of the magnitudes $|(g_0/\rho_0)\nabla\rho|$ in the unit of Eotvos (E) (1 E = $10^{-9}$ $s^{-2}$) at the four levels ( z = 0, -500 m, -1,000 m, and -2,000 m).

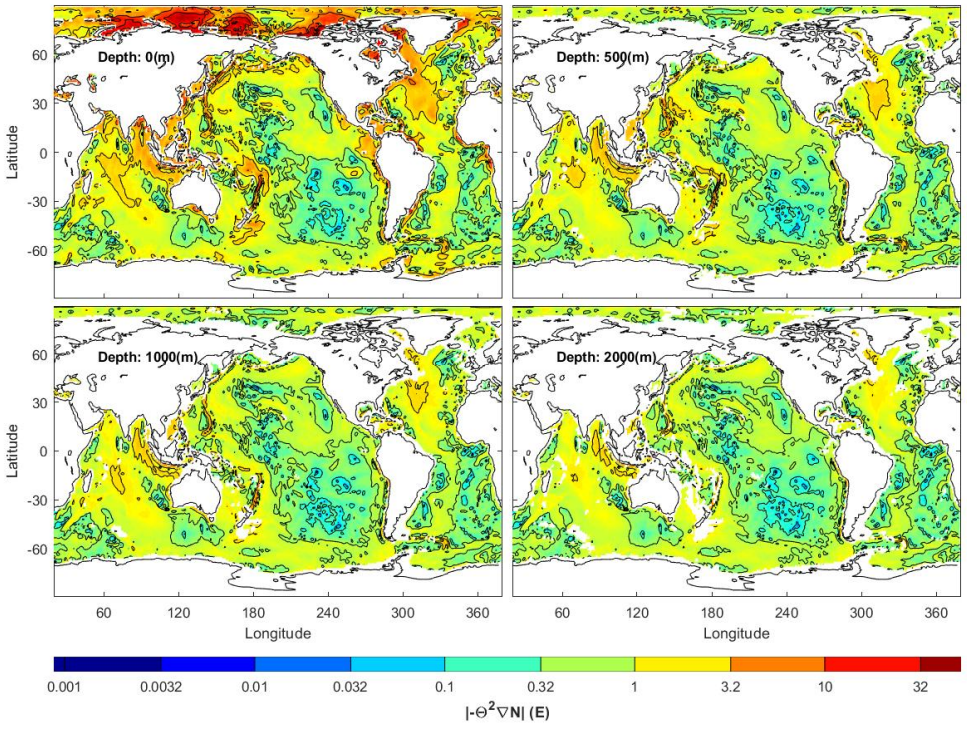


**Figure 9.** Horizontal contour plots of the magnitudes $|\Theta^2\nabla N|$ in the unit of Eotvos (E) (1 E = $10^{-9}$ $s^{-2}$) at the four levels ( z = 0, -500 m, -1,000 m, and -2,000 m).

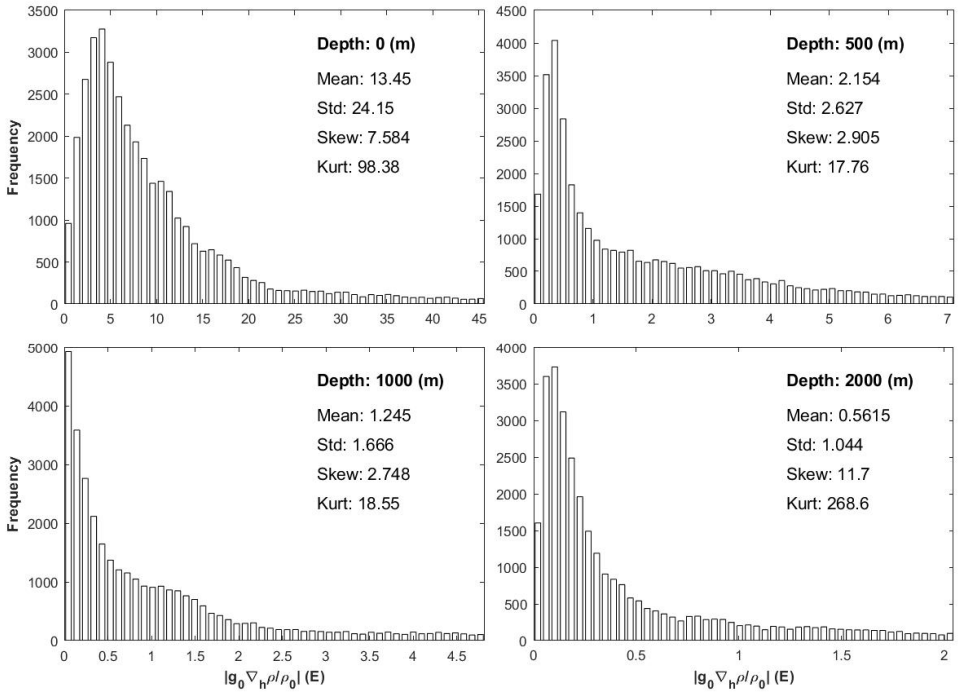


**Figure 10.** Histograms of the magnitudes $|(g_0/\rho_0)\nabla\rho|$ in the unit of Eotvos (E) ($1\ E = 10^{-9}\ s^{-2}$) at the four levels (z = 0, -500 m, -1,000 m, and -2,000 m).

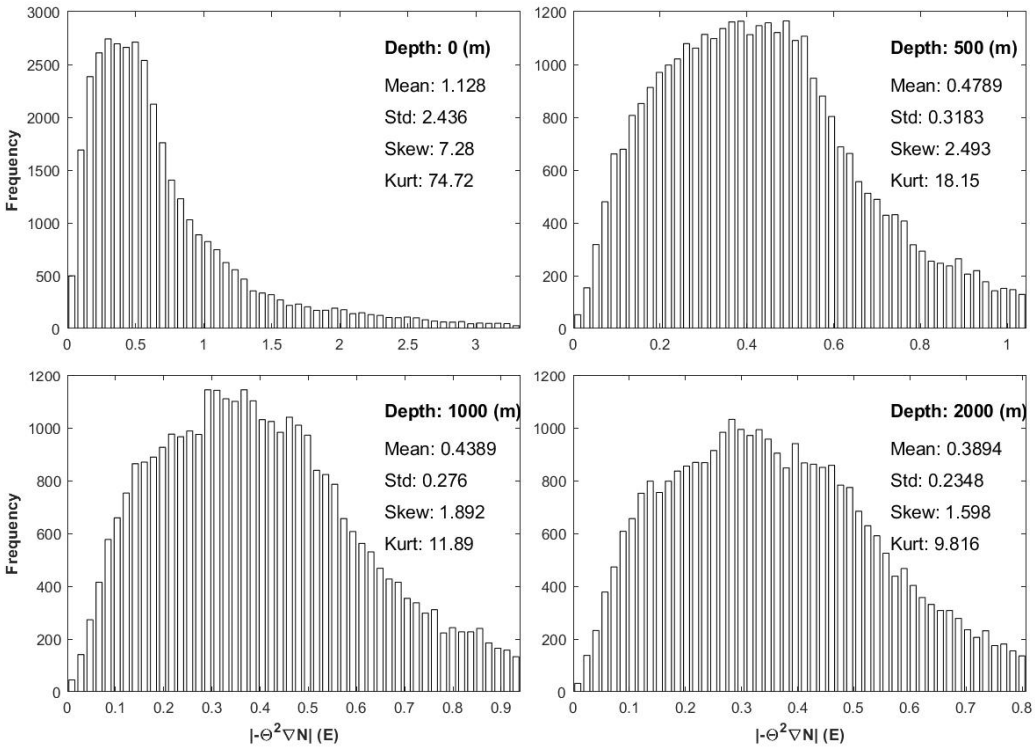


**Figure 11.** Histograms of the magnitudes $|\Theta^2\nabla N|$ in the unit of Eotvos (E) ($1\ E = 10^{-9}\ s^{-2}$) at the four levels (z = 0, -500 m, -1,000 m, and -2,000 m).

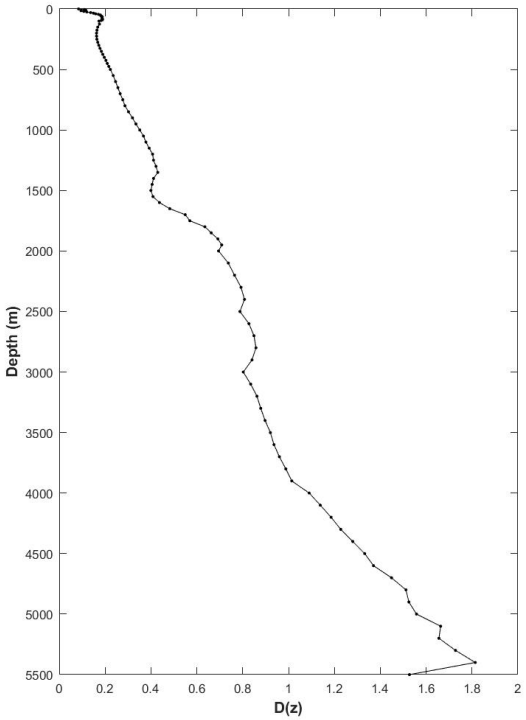


**Figure 12.** Depth dependent *D*-number calculated from the EIGEN-6C4 and WOA18 datasets.

## 8 1½ Layered Model with Rigid Lid

A 1½ layered model with rigid lid (Figure 13a) is used to test the effect of the horizontal gravity disturbance vector ($g_0\nabla N$) on the ocean circulation. This model contains two constant density layers with the upper layer of density $\rho_1$ above the thermocline and lower layer of density $\rho_2$ below the thermocline. Let the water depth be represented by $H(\lambda, \varphi)$, and the upper thickness be $h(\lambda, \varphi)$. The lower layer thickness is represented by $[H(\lambda, \varphi) - h(\lambda, \varphi)]$. The lower layer is assumed motionless, and the upper layer is in motion with the velocity of **U**. This 1½ layered model is often used to predict and simulate the wind-driven circulation mostly confined to upper oceans above the thermocline.

Let the atmospheric pressure at $z = 0$ be represented by $p_a(\lambda, \varphi)$. Vertical integration of hydrostatic balanced equation (42) from $z = 0$ down to $z$ in the upper layer gives

$$\hat{p}_1 = p_a + \rho_0 g_0 (z - N) - (\rho_1 - \rho_0) g_0 z, \quad 0 \geq z \geq -h \tag{46}$$

and lower layer

$$\hat{p}_2 = p_a + \rho_0 g_0 (z - N) + (\rho_1 - \rho_0) g_0 h - (\rho_2 - \rho_0) g_0 (z + h), \quad -h \geq z \geq -H \tag{47}$$

Since the lower layer is motionless, the driving force in (41) should be zero,

$$-\nabla \hat{p}_2 + (\rho_2 - \rho_0)\, g_0 \nabla N = 0, \quad -h \geq z \geq -H \tag{48}$$

and so as for the friction forces, $\mathbf{F}_h = 0$, and $\mathbf{F}_v = 0$. Elimination of $\hat{p}_2$ from (47) and (48) leads to

$$\nabla p_a = \rho_2 g_0 \nabla N + (\rho_2 - \rho_1) g_0 \nabla h \tag{49}$$

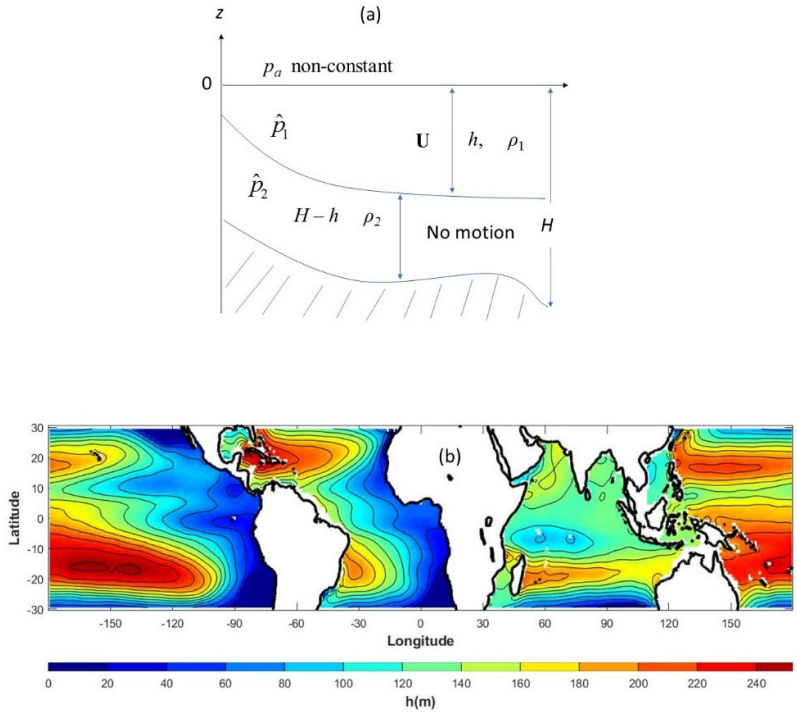


438

439 **Figure 13.** (a) A 1½ layer model with the rigid lid, and (b) climatological annual mean 20°C
440 isotherm depth ($h$) in tropical regions (30°S – 30°N) identified from WOA18 annual mean
441 temperature data.

442

443 Elimination of $p_a$ from (46) and (49) leads to

444 $$\nabla \hat{p}_1 = (\rho_2 - \rho_0) g_0 \nabla N + (\rho_2 - \rho_1) g_0 \nabla h, \quad 0 \geq z \geq -h \tag{50}$$

445 Substitution of (50) into (41) for the upper layer gives,

446 $$\boxed{\left[ \frac{D\mathbf{U}}{Dt} + f\mathbf{k} \times \mathbf{U} \right] = -g' \nabla h - g' \nabla N + (\mathbf{F}_h + \mathbf{F}_v)} \tag{51}$$

447 where

448 $$g' = \frac{\rho_2 - \rho_1}{\rho_0} g_0 = O(10^{-2}\ \mathrm{m\ s^{-2}})$$

449 is the reduced gravity. The continuity equation is given by,

450 $$\frac{\partial h}{\partial t} + \nabla \bullet (h\mathbf{U}) = 0 \tag{52}$$

451 Vertical integration of (51) from $z = 0$ down to $z = -h$ gives

452 $$h\left( \frac{D\mathbf{U}}{Dt} + f\mathbf{k} \times \mathbf{U} \right) = -g' h \nabla h - g' h \nabla N + \frac{\boldsymbol{\tau}}{\rho_0} - \gamma h \mathbf{U} + A h \nabla^2 \mathbf{U} \tag{53}$$

453 where (36), (37), and (38) are used.

Importance of the horizontal gravity disturbance vector ($g_0\nabla N$) on the ocean circulation can be identified by the comparison between $\nabla N$ and $\nabla h$ with the non-dimensional $B$ number,

$$B = \frac{O(|\nabla N|)}{O(|\nabla h|)} \approx \frac{\text{mean }(|\nabla N|)}{\text{mean }(|\nabla h|)} \tag{54}$$

and between $(-g'h\nabla N)$ and $(\boldsymbol{\tau}/\rho_0)$ with the non-dimensional $F_1$ number,

$$F_1 = \frac{O(\rho_0 g'h|\nabla N|)}{O(|\boldsymbol{\tau}|)} \approx \frac{\text{mean }(\rho_0 g'h|\nabla N|)}{\text{mean }(|\boldsymbol{\tau}|)} \tag{55}$$

In tropical oceans (20°S – 20°N), the depth $h$ in the 1½ layer model (Figure 13a) is the pycnocline depth, which is commonly represented by the 20°C isotherm depth (Kessler 1990). The WOA18 annual mean 1°×1° temperature data are used to identify the 20°C isotherm depth $h$ (shown in Figure 13b), which is comparable to the Climate Diagnostics Bulletin on the depth of 20°C isotherm from the NOAA/Climate Prediction Center for the tropical Pacific Ocean (see https://www.cpc.ncep.noaa.gov/products/analysis_monitoring/bulletin_tmp/figt16.gif.)

The annual mean $h$ data are used to compute $|\nabla h|$ (Figure 14a). The static gravity field model EIGEN-6C4 $N$ data are used to calculate $|\nabla N|$ (Figure 14b). The histogram of $|\nabla h|$ shows a positively skewed distribution with the mean of $6.882\times10^{-5}$ (Figure 14c). The histogram of $|\nabla N|$ also show positively skewed distributions with the mean of $1.764\times10^{-5}$ (Figure 14d). The $B$ number is 25.63% using Eq (54).

The absolute values of the surface wind stress $|\boldsymbol{\tau}|$ (Figure 15a) are from the SMD94 annual mean surface wind stress ($\boldsymbol{\tau}$) data. The annual mean $h$ data and the static gravity field model EIGEN-6C4 $N$ data are used to calculate $\rho_0 g'h|\nabla N|$ (Figure 15b). The histograms of $|\boldsymbol{\tau}|$ (Figure 15c) and $\rho_0 g'h|\nabla N|$ (Figure 15d) are quite different with much less skewness for $|\boldsymbol{\tau}|$ than for $\rho_0 g'h|\nabla N|$. The mean of $|\boldsymbol{\tau}|$ is 0.06072 $Nm^{-2}$. The mean of $\rho_0 g'h|\nabla N|$ is 0.02283 $Nm^{-2}$. Therefore, the $F_1$ number is 37.6% using Eq (55). Both $B$ number (26.63%) and $F_1$ number (37.6%) evidently show the importance of the gravity disturbance vector ($g_0\nabla N$) in the 1½ layer model dynamics in comparison to the horizontal gradient of the upper layer thickness $|\nabla h|$ and the absolute values of the surface wind stress $|\boldsymbol{\tau}|$.

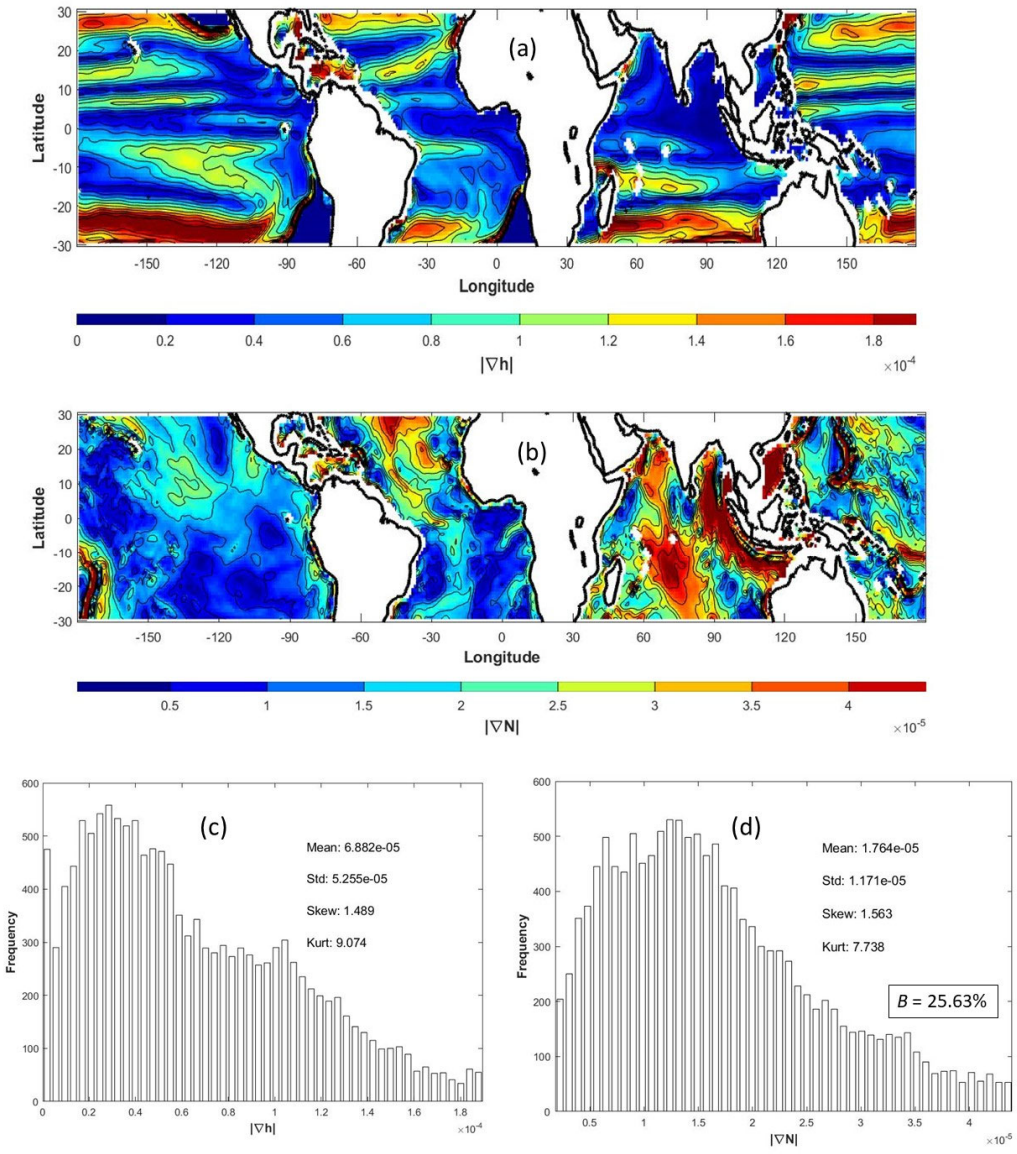


**Figure 14.** Contour plots of (a) $|\nabla h|$ and (b) $|\nabla N|$ as well as histograms of (c) $|\nabla h|$ and (d) $|\nabla N|$ in the tropical regions (30°S – 30°N).

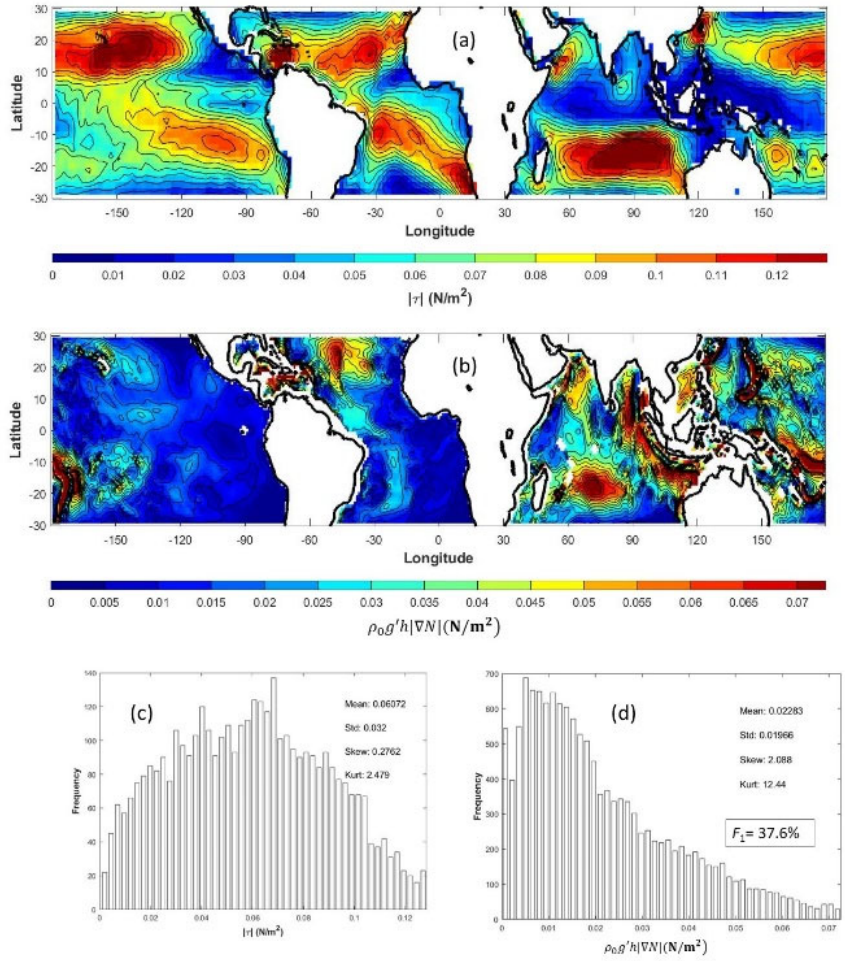


**Figure 15.** Contour plots of (a) $|\boldsymbol{\tau}|$ and (b) $\rho_0 g' h|\nabla N|$ (unit: N/m$^2$) as well as histograms of (c) $|\boldsymbol{\tau}|$ and (d) $\rho_0 g' h|\nabla N|$ in the tropical regions (30°S – 30°N).

## 9. Combined Sverdrup-Stommel-Munk dynamics

For steady-state low Rossby number flow with friction (i.e., $D\mathbf{U}/Dt = 0$, and $\mathbf{F}_h \neq 0$, $\mathbf{F}_v \neq 0$), Eq (41) is simplified into

$$\rho_0\left[f\mathbf{k}\times\mathbf{U} - A\nabla^2\mathbf{U} - \frac{\partial}{\partial z}\left(K\frac{\partial \mathbf{U}}{\partial z}\right)\right] = -\nabla\hat{p} + \left(\rho-\rho_0\right)g_0\nabla N \tag{56}$$

where Eq (36) is used for $\mathbf{F}_h$ and $\mathbf{F}_v$. Vertical integration of (56) from $z = -H$ to $z = 0$ and use of Eq (37) and Eq (38) leads to

$$\left[f\mathbf{k}\times\mathbf{M} - A\nabla^2\mathbf{M} - \left(\boldsymbol{\tau} - \gamma\mathbf{M}\right)\right] = -\int_{-H}^{0}\nabla\hat{p}dz + \int_{-H}^{0}\left[\left(\rho-\rho_0\right)g_0\nabla N\right]dz \tag{57}$$

Curl of the vector equation (57) gives,

$$\nabla\times\left[f\mathbf{k}\times\mathbf{M} - A\nabla^2\mathbf{M} - \left(\boldsymbol{\tau} - \gamma\mathbf{M}\right)\right] = g_0\int_{-H}^{0}\left[\nabla\rho\times\nabla N\right]dz \tag{58}$$

Let the volume transport stream-function ($\Psi$) be defined by

$$\nabla\Psi = -\frac{1}{\rho_0}\mathbf{k}\times\mathbf{M}, \qquad \text{i.e., } \mathbf{M} = \rho_0\mathbf{k}\times\nabla\Psi \tag{59}$$

Substitution of (59) into (58) leads to

$$\nabla\times\left[-f\nabla\Psi - A\nabla^2\left(\mathbf{k}\times\nabla\Psi\right)+\gamma\left(\mathbf{k}\times\nabla\Psi\right)\right] = \frac{1}{\rho_0}\left[\nabla\times\boldsymbol{\tau} + g_0\int_{-H}^{0}\left(\nabla\rho\times\nabla N\right)dz\right] \tag{60}$$

Since

$$\nabla\times\left(\mathbf{k}\times\nabla\Psi\right) = \mathbf{k}\nabla^2\Psi,\ \nabla\times(-f\nabla\Psi) = \beta\frac{\partial\Psi}{\partial x},\ \ \beta\equiv\frac{df}{dy}\ \ (\beta \text{ coefficient}) \tag{61}$$

where ($x$, $y$) are local horizontal coordinates corresponding to the spherical geopotential coordinates with the $x$-axis pointing east-west, and the y-axis pointing north-south. Substituting (61) into (60) and conducting inner product with the unit vector **k**, we obtain a combined Sverdrup-Stommel-Munk equation using the true gravity,

$$\boxed{-A\nabla^4\Psi + \gamma\nabla^2\Psi + \beta\frac{\partial\Psi}{\partial x} = \frac{1}{\rho_0}\left[\text{curl}\,\boldsymbol{\tau} + g_0\int_{-H}^{0}\mathbf{k}\bullet\left(\nabla\rho\times\nabla N\right)dz\right]} \tag{62}$$

which has an additional horizontal gravity disturbance vector forcing (GDVF) term,

$$\text{GDVF} = g_0\int_{-H}^{0}\mathbf{k}\bullet\left(\nabla\rho\times\nabla N\right)dz = g_0\int_{-H}^{0}J(\rho,N)dz \tag{63}$$

Here, $J(\rho,N) = (\partial\rho/\partial x)(\partial N/\partial y) - (\partial N/\partial x)(\partial\rho/\partial y)$, is the Jacobian of $\rho$ and $N$. Eq (62) is reduced to Eq.(5.5.29) in Pedlosky (1984) when the horizontal gravity disturbance vector vanishes. After changing the flat lower boundary into non-flat bottom topography, $z = -H(x, y)$, Eq (62) becomes,

$$-A\nabla^4\Psi + \gamma\nabla^2\Psi + \beta\frac{\partial\Psi}{\partial x} = \frac{1}{\rho_0}\left[\text{curl}\,\boldsymbol{\tau} + g_0\int_{-H(x,y)}^{0}J(\rho,N)dz\right] + \begin{matrix}\text{Bottom Topographic}\\ \text{Effect Term}\end{matrix} \tag{64}$$

Note that the bottom topographic effect on the volume transport is beyond the scope of this study, and therefore is not identified.

A non-dimensional number $F_2$ is defined by,

$$F_2 = \frac{O\left[\left|\text{GDVF}\right|\right]}{O\left[\left|\text{curl}\,\boldsymbol{\tau}\right|\right]} \approx \frac{\text{Mean}\left[\left|\text{GDVF}\right|\right]}{\text{Mean}\left[\left|\text{curl}\,\boldsymbol{\tau}\right|\right]} \tag{65}$$

to identify the importance of GDVF versus the surface wind stress curl. The GDVF is calculated by Eq (63) using the density $\rho$ from the WOA18 annual mean temperature and salinity data and the true-geoid undulation $N$ from the EIGEN-6C4 data. The surface wind stress curl is computed from the SMD94 annual mean surface wind stress ($\boldsymbol{\tau}$) data.

The calculated global GDVF (simplified as 'J' in Figure 16) and surface wind stress curl (Figure 17) have comparable magnitudes with different horizontal distributions (Figures 16a and 17a). The histograms of |GDVF| (Figure 16b) and (|curl $\boldsymbol{\tau}$|) (Figure 17b) show near Gamma distribution. |GDVF| has comparable mean and standard deviation (3.448,

4.283)×10$^{-8}$Nm$^{-3}$, with |curl $\boldsymbol{\tau}$| (4.984, 4.052)×10$^{-8}$ Nm$^{-3}$; but has two-time larger skewness and kurtosis (2.19, 8.12), than |curl $\boldsymbol{\tau}$| (1.081, 4.137). The $F_2$ number is 69.18%. Note that large |GDVF| values occurring around the Gulf Stream and Antarctic Circumpolar Circulation regions. The reason is explained as follows. From Eq (63) the GDVF can be rewritten by

$$\mathrm{GDVF} = \mathbf{k} \bullet \left( \mathbf{B} \times g_0 \nabla N \right) = g_0 \left| \mathbf{B} \right| \left| \nabla N \right| \sin \alpha, \quad \mathbf{B} \equiv \int_{-H}^{0} \nabla \rho dz \tag{66}$$

where the vector **B** represents the baroclinicity; and α is the angle between **B** and $\nabla N$. The |GDVF| value depends on the angle α and the intensities of the two vectors |**B**| and |$\nabla N$|. Near the Gulf Stream and Antarctic Circumpolar Circulation regions, vector **B** is in the north-south direction usually with large magnitude. However, $\nabla N$ is in the east-west direction (Figure 7) with noticeable magnitude (i.e., |$\nabla N$|). Near 90° cross angle α may be the major reason to cause large |GDVF| values there. The $F_2$ number (69.18%) demonstrates that the GDVF is comparable to the surface wind forcing (curl $\boldsymbol{\tau}$) in the combined Sverdrup-Stommel-Munk dynamics.

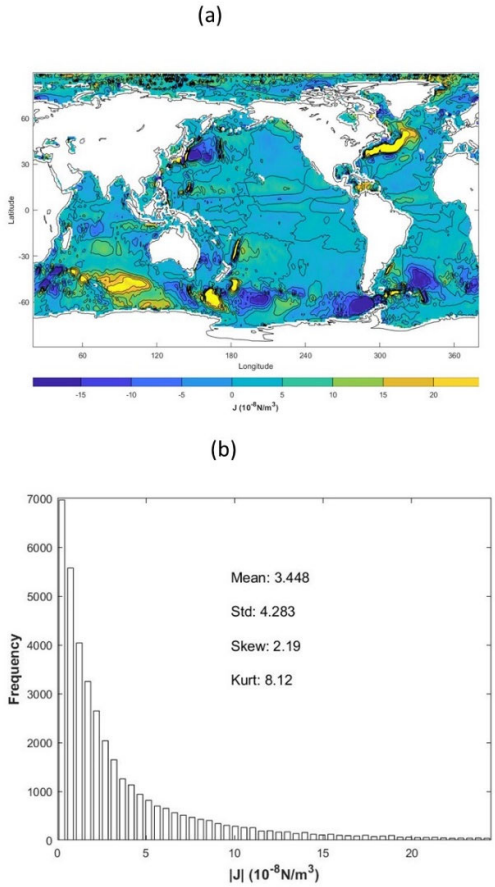


**Figure 16.** (a) Contour plot of climatological annual mean GDVF (unit: 10$^{-8}$ Nm$^{-3}$) calculated using the NOAA/NCEI WOA18 annual mean temperature and salinity data and the EIGEN-6C4 geoid undulation (*N*) data, and (b) histogram of |GDVF|. Note that GDVF is simplified by 'J' here.

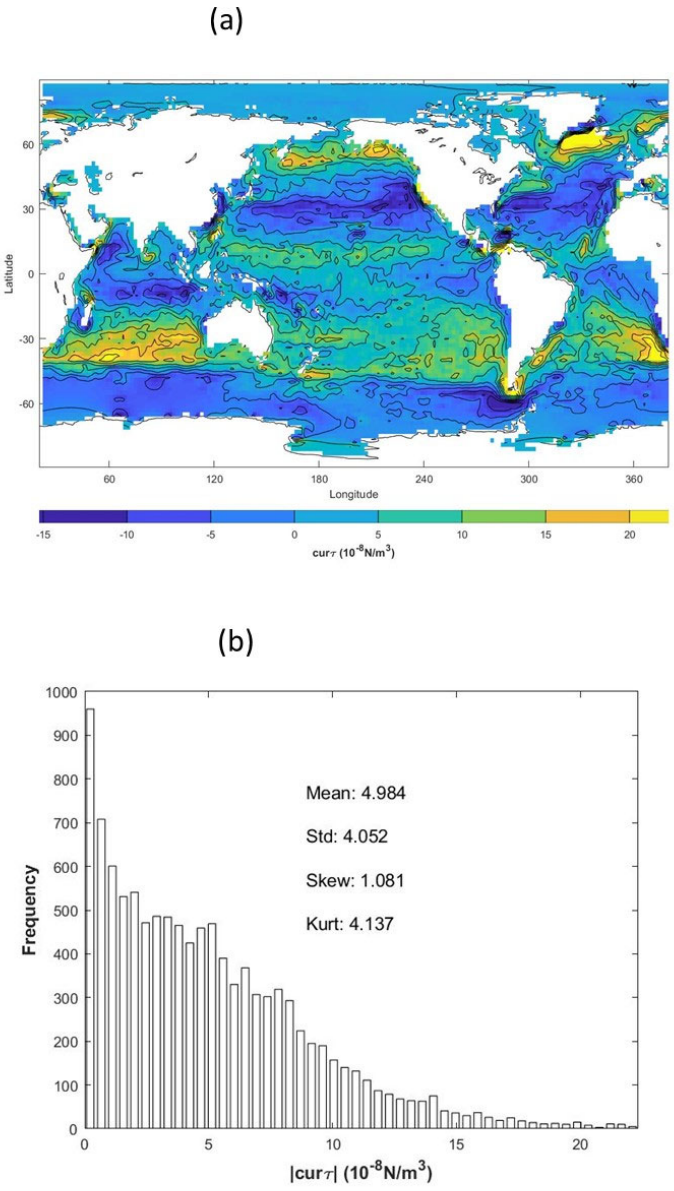


**Figure 17.** Climatological annual mean (curl τ) (unit: $10^{-8}$ $Nm^{-3}$) calculated using the SMD94 data: (a) contour plot of (curl $\boldsymbol{\tau}$), and (b) histogram of |curl $\boldsymbol{\tau}$|.

## 10. New Spheroidal and Spherical Geopotential Approximations

Sections 7-9 show that the difference in horizontal pressure gradient force between using the true and spherical geopotential coordinates, i.e., the horizontal gravity disturbance vector ($g_0\nabla N$), is comparable to the other forcing terms such as Coriolis force, surface winds, and horizontal pressure gradient force. Table 2 summarizes the differences in the metric terms and the horizontal pressure gradient force among using the spherical, spheroidal, and true geopotential coordinates and shows the horizontal gravity disturbance vector ($g_0\nabla N$) non-negligible in the spheroidal and spherical geopotential coordinates using the true geopotential

562 (i.e., true gravity $\mathbf{g}_t$.) Thus, new spheroidal and spherical geopotential approximations are
563 proposed:

> After adding the horizontal gravity disturbance vector ($g_0\nabla_e N$) or ($g_0\nabla_s N$) in the horizontal
564 equation of motion, the spheroidal or spherical geopotential coordinates can be used for the true geopotental (i.e., true gravity $\mathbf{g}_t$.)

565 It might be the most feasible and effective way to accept these two approximations for the
566 ocean dynamics using the true geopotential (i.e., true gravity $\mathbf{g}_t$) and keeping the existing
567 model framework.
568
569 **Table 2**. Metric terms and horizontal pressure gradient differences due to the transformation
570 among the true, spheroidal, and spherical geopotential coordinates.

| | Metric Terms | Horizontal Pressure Gradient | Total Difference |
|---|---|---|---|
| True to Spheroidal | $\varepsilon_{t\to e}^{(m)} \approx 0$ Negligible | $g_0\nabla_e N$ Non-Negligible | $\varepsilon_{t\to e}^{(m)} + g_0\nabla_e N$ Non-Negligible |
| True to Spherical | $\varepsilon_{t\to e}^{(m)} + \varepsilon_{e\to s}^{(m)} \approx 0$ Negligible | $g_0\nabla_e N + \varepsilon_{e\to s}^{(p)}$ Non-Negligible | $\varepsilon_{t\to e}^{(m)} + \varepsilon_{e\to s}^{(m)} + \varepsilon_{e\to s}^{(p)} + g_0\nabla_e N$ Non-Negligible |
| Spheroidal to Spherical | $\varepsilon_{e\to s}^{(m)} \approx 0$ Negligible | $\varepsilon_{e\to s}^{(p)} \approx 0$ Negligible | $\varepsilon_{e\to s}^{(m)} + \varepsilon_{e\to s}^{(p)} \approx 0$ Negligible |

571

572 **11. Conclusions**

573 This paper takes an alternative approach using the relationships among the spherical,
574 spheroidal, and true geopotential coordinates to further confirm the importance of the
575 horizontal gravity disturbance vector ($g_0\nabla N$) in oceanic dynamics. Difference among the
576 spheroidal, spherical, and true geopotential coordinates has two types: metric terms and
577 horizontal pressure gradient force. The difference in the metric terms is negligible among the
578 three geopotential coordinates (Gill 1982, CW22, CWSM23). The difference in the
579 horizontal pressure gradient force between the spheroidal and spherical is also negligible
580 (Gates 2004, Beńard 2015, Staniforth 2015). However, the difference in the horizontal
581 pressure gradient force between the true and spheroidal/spherical geopotential coordinates is
582 the horizontal gravity disturbance vector ($g_0\nabla N$).
583 Effect of the gravity disturbance vector in ocean dynamics is demonstrated by the newly
584 derived geostrophic and thermal wind relation, 1½ layer model, and combined Svedrup-
585 Stommel-Munk equation through using true-geopotential (i.e., true gravity $\mathbf{g}_t$) in the spherical

geopotential coordinates, i.e., adding $g_0\nabla N$ in the horizontal equation of motion. The depth dependent nondimensional *D*-number and depth independent nondimensional (B, $F_1$, $F_2$) numbers are defined to identify the importance of gravity disturbance vector forcing versus the horizontal density gradient in the thermal wind relation (D-number), versus the horizontal gradient of upper layer thickness in 1½ layer model (B-number), versus the surface wind stress in 1½ layer model ($F_1$-numbers), and versus the surface wind stress curl in the combined Sverdrup-Stommel-Munk equation ($F_2$-number). Using three publicly available datasets in climatological, geodetic, and oceanographic communities (SMD94, EIGEN-6C4, WOA18), the D-number increases with depth almost monotonically from 8.4% at z = 0, 22.2% at z = -500 m, 35.3% at z = -1,000 m, 69.3% at z = -2,000 m, 81.4% at z = -3,000 m, 108.7% at z = -4,000 m, 157.6% at z = -5,000 m; the B-number is 25.92%; the $F_1$-number is 37.6%; and the $F_2$-number is 69.18%. It clearly shows the horizontal gravity disturbance vector forcing comparable to the traditional forcing factors such as the horizontal density gradient, surface wind stress, and surface wind stress curl in ocean dynamics.

With such an evidence, the current spheroidal and spherical geopotential approximations should be revised for using the true geopotential in ocean dynamics just adding a phrase "including the horizontal gravity disturbance vector in the existing horizontal equation of motion." In other words, it is urgent to include the horizontal gravity disturbance vector ($g_0\nabla N$) in any analytical or numerical oceanic models.

**Acknowledgments**

Mr. Chenwu Fan's computational assistance is highly appreciated. The EIGEN-6C4 geoid undulation [$N(\lambda, \varphi)$] data was provided by the International Centre for Global Earth Models (ICGEM). The WOA18 annual mean temperature and salinity for the density $\rho$ data was obtained from the NOAA/NCEI. The SMD94 annual mean wind stress ($\boldsymbol{\tau}$) data was archived from the International Research Institute for Climate and Society.

**Funding**

This research received no external funding.

**Open Research (Data Availability Statement)**

The data used in this paper are publicly available with the geoid (*N*) from the ICGEM global static gravity model EIGEN-6C4 at http://icgem.gfz-potsdam.de/home, the density $\rho$ data from the WOA18 annual mean temperature and salinity at https://www.ncei.noaa.gov/access/world-ocean-atlas-2018/, and the SMD94 annual mean wind stress ($\boldsymbol{\tau}$) data at https://iridl.ldeo.columbia.edu/SOURCES/.DASILVA/.

## Appendix A. Major mistakes in CW22, SM22, CWSM23, and additional comments by Chang (in Appendix B)

Major mistakes in CWSM23 (https://www.sciencedirect.com/science/article/pii/S0377026523000337), CW22 (https://www.nature.com/articles/s41598-022-09967-3), CW22 Supplementary (https://static-content.springer.com/esm/art%3A10.1038%2Fs41598-022-09967-3/MediaObjects/41598_2022_9967_MOESM1_ESM.pdf), SM22 (https://www.nature.com/articles/s41598-022-10023-3), SM22 Supplementary (https://static-content.springer.com/esm/art%3A10.1038%2Fs41598-022-10023-3/MediaObjects/41598_2022_10023_MOESM1_ESM.pdf), and additional comments by Chang to DAO (Appendix B) have been identified. The materials inside the boxes are directly copied from CW22, SM22, CWSM23, and Appendix B.

### *A1. Wrong comparison leads to wrong statement of "negligible impact of δg".*

SM22 use the following equations,

$$\rho_0 \frac{D\mathbf{U}}{Dt} + \rho_0 f\mathbf{k}\times\mathbf{U} + \nabla_h p = \rho\nabla_h V + \rho_0\mathbf{F} \quad \text{Eq(1) in SM22}$$

Horizontal gravity

$$V \approx g_0(N - z) \quad \text{Eq(3) in SM22}$$

$$\rho_0 \frac{D\mathbf{U}}{Dt} + \rho_0 f\mathbf{k}\times\mathbf{U} - \rho_0\mathbf{F} = g_0 \int_{z'=S}^{z'=z} \nabla_h \rho dz' - \rho_0 g_0 \nabla_h (S - N) + g_0(\rho - \rho_0)\nabla_h N \quad \text{Eq(5) in SM22}$$

Baroclinic presure gradient — Surface pressure gradient — Horizontal gravity anomaly

to claim that

> At the surface z = S the "horizontal gravity anomaly" term is zero by construction because ρ = $\rho_0$. In the subsurface, while the "horizontal gravity anomaly" term in (5) is non-zero, it is approximately three orders of magnitude smaller than the "horizontal gravity" term in (1).....
> Consequently, "horizontal gravity" would likely have a negligible impact on ocean circulation even in a model formulated in absolute spherical coordinates.

Anyone with basic scientific knowledge knows that the importance of a forcing term in atmospheric and oceanic dynamics should be compared to other terms *in the same dynamic equation*. SM22 compared $[g_0(\rho - \rho_0)\nabla_h N]$ in [Eq (5) SM22] to $[g_0\rho\nabla_h N]$ in [Eq (1) SM22]. Such comparison is meaningless and wrong. The correct comparison should be between the horizontal gravity anomaly $[g_0(\rho - \rho_0)\nabla_h N]$ and the baroclinic pressure

651 gradient $g_0\int_{z'=S}^{z'=z}\nabla_h\rho dz'$ in [Eq (5) SM22]. A minor issue is that $\rho_0$ is a constant (e.g., 1028

652 kg/m$^3$), not the surface density.

653

654 ***A2. The statement on "shift in the reference density in oceanic Ekman layer" is wrong***.

655

656 SM22 use the following four equations,

Four Equations in SW22 Supplementary ($\nabla_h$ is the horizontal vector differential operator)

$$\int_z^0 \mathbf{U}dz' = \underbrace{\frac{1}{\rho_0 f}\int_z^0 \mathbf{k}\times\nabla_h\hat{p}dz'}_{\text{Pressure Gradient}} + \underbrace{\frac{1}{f}\int_z^0 b\mathbf{k}\times\nabla_h N dz'}_{\text{Gravity Disturbance}} \underbrace{-\frac{\mathbf{k}\times\boldsymbol{\tau}}{\rho_0 f}}_{\text{Wind Stress (Ekman)}} \quad \text{(13) in SM22 Suppl}$$

Total

$$b^* = -g_0(\rho-\rho_0^*)/\rho_0^* \approx b+\delta b_0,\quad \delta b_0 = g_0\delta\rho_0/\rho_0^* \quad \text{(14) in SM22 Suppl}$$

657

$$\int_z^0 \mathbf{U}dz' = \underbrace{\frac{1}{\rho_0 f}\int_z^0 \mathbf{k}\times\nabla_h\hat{p}^* dz'}_{\text{Pressure Gradient}} + \underbrace{\frac{1}{f}\int_z^0 b\mathbf{k}\times\nabla_h N dz' - z\frac{\delta b_0}{f}\mathbf{k}\times\nabla_h N}_{\text{Gravity Disturbance}} \underbrace{-\frac{\mathbf{k}\times\boldsymbol{\tau}}{\rho_0 f}}_{\text{Wind Stress (Ekman)}} \quad (15)$$

Total

$$\nabla_h\hat{p} = \nabla_h\hat{p}^* + g_0\delta\rho_0\nabla_h N \quad \text{(16) in SM22 Suppl}$$

Here, $\rho$ is the density; $b=-g_0(\rho-\rho_0)/\rho_0$, is the buoyancy;
$(\rho_0^*,\ b^*, \hat{p}^*)$ are the shifted $(\rho_0, b, \hat{p})$ due to $\delta\rho_0$

658 to claim that:

> An arbitrary change in the reference density leads to a vertically-uniform addition to the "horizontal gravity"-driven component of the flow, and thus a vertically-integrated
> 659 transport that increases linearly with depth. This implies that the "horizontal gravity"-driven component of the flow is ill-defined, and thus that analyzing this flow in isolation, or as part of the 'Ekman' transport (as done by Chu[1]) is misleading.

660 [Eq(15) SM22 Supplementary] has two severe errors: (1) the sign for the term
661 $z(\delta b_0/f)\mathbf{k}\times\nabla_h N$ should be '+' not '-'; (2) the buoyancy $b$ in [Eq.(15) SM22
662 Supplementary] is based on the unshifted reference density $\rho_0$, but the dynamic pressure $\hat{p}^*$
663 is based on the shifted reference density $\rho_0^*$.

664 If the shifted reference density $\rho_0^*$ is used for both buoyancy $b$ and dynamic pressure $\hat{p}$,
665 and the sign for the term $z(\delta b_0/f)\mathbf{k}\times\nabla_h N$ is corrected from '-' to '+', [Eq.(15) SM22
666 Supplementary] becomes [substitution of Eq.(14) into Eq.(15) in SM22 Supplementary]

667 $$\underset{\text{Total}}{\int_z^0 \mathbf{U}dz'} = \underset{\text{Pressure Gradient}}{\frac{1}{\rho_0 f}\int_z^0 \mathbf{k}\times\nabla_h \hat{p}^* dz'} + \underset{\text{Gravity Disturbance}}{\frac{1}{f}\int_z^0 b^*\mathbf{k}\times\nabla_h N dz'} - \underset{\text{Wind Stress (Ekman)}}{\frac{\mathbf{k}\times\boldsymbol{\tau}}{\rho_0 f}} \quad \text{(A1)}$$

668 which shows that the Ekman transport driven by the horizontal gravity disturbance vector is
669 *well-defined*, and there is no vertically integrated transport that increases linearly with depth.

670 ***A3. The statement on "shift to absolute spherical coordinates in atmospheric Ekman***
671 ***layer" is wrong***.

672 SM22 Supplementary used the following equations,

| | |
|---|---|
| $\rho = \rho_0 + \tilde{\rho}$ | (5) in SM22 Supplementary |
| $\mathbf{F} = \frac{\partial}{\partial z}(K\frac{\partial \mathbf{U}}{\partial z})$ | (10) in SM22 Supplementary |
| 673 $\rho_0 f\mathbf{k}\times\mathbf{U} + \nabla_3 p \approx \rho(z)\mathbf{g} + \rho_0\mathbf{F}$ | (20) in SM22 Supplementary |
| $\rho_0 f\mathbf{k}\times\mathbf{U}_g = -\nabla_h p + \rho(z)\mathbf{g}_h,\ \mathbf{g}_h \equiv \delta\mathbf{g}$ | (24) in SM22 Supplementary |
| $\rho_0 f\mathbf{k}\times(\mathbf{U}-\mathbf{U}_g) = \rho_0\mathbf{F}$ | (25) in SM22 Supplementary |

674 to claim that

675 Thus the "Ekman" flow and pumping are unchanged by the shift to absolute spherical coordinates.

676 SM22 mistakenly or intentionally treats the atmospheric density $\rho$ as a constant. In fact,
677 the atmospheric density varies with $z$ [see Eq (23) in Chu 2021c]:

678 $$\frac{\rho}{\rho_0} = s(z),\ \ s(z) \equiv \exp\left(-\frac{z}{H}\right),\quad H = 10.4 \text{ km} \quad \text{(A2)}$$

679 Anyone with basic knowledge on college ordinary differential equations knows that solution
680 of a linear ordinary differential equation is invariant with the shift of the independent variable
681 *only if all the coefficients in the equation are constants*; but is variant even if even only one
682 coefficient is not constant (i.e., a function of the independent variable). [Eq (25) in SM
683 Supplementary] is a second order ordinary differential equation with **U** the dependent
684 variable, and $z$ the independent variable, and ($K$, $\mathbf{U}_g$) the coefficients.

685 In the classical atmospheric Ekman layer dynamics, there is no gravity disturbance vector
686 $\delta\mathbf{g} = 0$, and the coefficients ($K, \nabla_h p$) are independent on $z$. This makes ($K$, $\mathbf{U}_g$) constants,
687 i.e., independent on $z$. Thus, the solution of [Eq (25) SM Supplementary] is invariant with
688 the shift to the absolute spherical coordinates (i.e., moving z-surfaces up and down).

689 However, with gravity disturbance vector $\delta\mathbf{g} \neq 0$, the term $\rho(z)\delta\mathbf{g}$ depends on z, and
690 so the coefficient $\mathbf{U}_g$ [from Eq.(24) SM Supplementary]. [Eq (25) in SM Supplementary] is
691 a second order ordinary differential equation with z-varying coefficient $\mathbf{U}_g$. The solution of
692 [Eq (25) in SM Supplementary] varies with the shift to the absolute spherical coordinates.

693 The Ekman flow and Ekman pumping change with the shift to absolute spherical coordinates
694 as shown in Chu (2021c). The gravity disturbance vector δ**g** *does affect* the atmospheric
695 Ekman flow and Ekman pumping.
696
697 ***A4. The metric terms are not the only difference between the spheroidal and true***
698 ***geopotential coordinates***.
699 The metric terms are treated as the only difference among the spheroidal, spherical, and
700 true geopotential coordinates in CW22, CWMS23, and Appendix B:

[see **(A) in Section B1 of Appendix B] →
So, what kind of approximation is needed for using this coordinate system?
If we examine (B1) carefully, all terms in the equation are local, except for the acceleration term, which involves how the coordinate axes change as a function of space As CW22 pointed out, in component form, the acceleration term can be written as:

$$\frac{DU}{Dt} = \mathbf{i}\frac{Du}{Dt} + \mathbf{j}\frac{Dv}{Dt} + \mathbf{k}\frac{Dw}{Dt} + u\frac{D\mathbf{i}}{Dt} + v\frac{D\mathbf{j}}{Dt} + w\frac{D\mathbf{k}}{Dt} \qquad (B2)$$

The last 3 terms in equation (B2) are the metric terms.
.....
Note that, as will be discussed below, for the irregular geopotential coordinate, other than the pressure gradient force and gravity, the horizontal components of the other 3 terms in equation (B1) can be evaluated on a spheroid that passes through the same point with only minor errors (relative error of the order of magnitude of the angle between the true geopotential surfaces and a spheroid,
701 which is of the order $10^{-4}$as estimated by CW22).

Line 13-17 in the Second Paragraph in CWSM23
As shown by CW22, the metric errors introduced in the calculus of the spheroidal geopotential approximation are small, reaffirming the long-standing practice of using
702 this coordinate system for atmospheric and oceanic modeling (Gill 1982, Staniforth 2022).
Based on these and similar analyses, CW22 and SM22 concluded that the horizontal components of the true gravity are not relevant to ocean (and atmospheric) dynamics because these horizontal components vanish when the coordinatesystemis interpreted correctly.

From the Second Paragraph on Page 2 in CW22:

Let us estimate how large this error might be. Mathematically, the exact form of the metric *terms is*[5] :

$$\frac{D\mathbf{U}}{Dt} = \mathbf{i}\frac{Du}{Dt} + \mathbf{j}\frac{Dv}{Dt} + \mathbf{k}\frac{Dw}{Dt} + u\frac{D\mathbf{i}}{Dt} + v\frac{D\mathbf{j}}{Dt} + w\frac{D\mathbf{k}}{Dt} \quad (4)$$

where u, v, w are the three velocity compnents, and i, j, and k are the three local unit vectors of the coordinate system. The last 3 terms on the RHS of (4) are the metric terms, which arise due to the local unit vectors changing direction following the fluid motion.

... This estimate confirms that the errors made by approximating the near oblate spheroidal coordinate in which the true gravity is exact vertical with a truely oblate shperoidal coordinate system is negligible, as suggested in ocean dynamics texts[3,4]

It is wrong because the difference in the horizontal pressure gradient force between the true and spheroidal/spherical geopotential coordinates exists in addition to the metric terms and is non-negligible (see Sections 2-3, and Table 2).

***A5. The scale analysis on the metric terms is meaningless.***

Since mistakenly neglecting the horizontal pressure gradient difference between the true and spheroidal geopotential coordinates, the scale analysis on the metric terms depicted in CW22 and the grey shaded paragraph [i.e., **(B) in Subsection B1 of Appendix B] is meaningless because the difference in the metric terms is negligible in comparison to the difference in the horizontal gradient force.

***A6. Mean sea level is mistakenly treated as geoid.***

MSL, time average of **observable** sea level, is defined in the American Meteorological Society (AMS) 's Glossary of Meteorology as "In the United States, mean sea level is defined as the mean height of the surface of the sea for all stages of the tide over a 19-year period. Selected values of mean sea level serve as the sea level datum for all elevation surveys in the United States https://glossary.ametsoc.org/wiki/Mean_sea_level." The MSL is defined by the World Meteorological Organization (WMO) as "The average sea surface level for all stages of the tide over a 19-year period, usually determined from hourly heights observed above a fixed reference level. Please see the WMO International Meteorological Vocabulary M0400 https://community.wmo.int/en/bookstore/international-meteorological-vocabulary for information.

The geoid, a **non-observable** surface, is inferred by a gravity field model as "The equipotential surface of the Earth's gravity field which best fits, in a least squares sense, global MSL https://geodesy.noaa.gov/GEOID/geoid_def.html)". The geoidal undulation relative to the Earth reference ellipsoid ranges from +85 m (Iceland) to −106 m (southern India Ocean) and is several orders of magnitude larger than the horizontal MSL variation. The following statement is wrong.

730

[see **(C) in Subsection B1 of Appendix B] →
However, in atmospheric and oceanic sciences, geopotential heights are computed with reference to the mean sea level (MSL), which is very close to a geoid but deviates from a reference ellipsoid. The MSL pressure (pressure on the hypothetical mean sea level which should coincide with a geoid if the ocean is motionless) is first computed, and then the
731 thickness is added to find the height of pressure surfaces above (or below) MSL, which practically is the distance of the upper level (or below sea-level) pressure surfaces from the mean sea level geoid. Hence the way that the geopotential heights are computed in practice means that the values are the height with respect to a reference geoid (the MSL) rather than the height with respect to a reference ellipsoid.

732

733

734 ***A7. The horizontal component of gravity does not vanish on the MSL.***

735 The following statement is wrong because MSL is NOT the geoid. The horizontal
736 component of gravity vanishes on the geoid but does not vanish on the MSL.

737

[see **(D) in Subsection B1 of Appendix B] →
On the MSL (a geoid), the horizontal component of gravity vanishes, hence the horizontal
738 static pressure gradient force that balances it also vanishes, and they continue to vanish on upper level "constant height" surfaces as long as the heights are computed with respect to the MSL surface (a geoid) rather than a hypothetical ellipsoid as assumed by the author ...

739

740 ***A8. The validity of proposed spheroidal geopotential approximation is never verified.***

741 Any approximation needs to be verified. However, the spheroidal geopotential
742 approximation proposed in CWSM23 has never been verified. Sections 2-3 and Table 2
743 show that the difference in horizontal gradient force from true to spheroidal geopotential
744 coordinates is non-negligible. Thus, the comments in the next two boxes are wrong. The
745 corrected spheroidal geopotential approximation is presented in Section 10.

First Paragraphy in CWSM23:

.....

Chang and Wolfe (2022; hereafter CW22) and Stewart and McWilliams (2022; hereafter SM22) pointed out that atmospheric and oceanic scientists express the equations of motion in coordinate form by defining the "vertical" direction in the coordinate system to be opposite to g, effectively using a geopotential coordinate (see, e.g., Gill 1982).

746 Importantly, in this coordinate system, the true gravity, $\mathbf{g}=\mathbf{g}_{\text{eff}}+\delta\mathbf{g}$, is exactly vertical—with no horizontal components. Furthermore, in this coordinate system, "horizontal" geopotential surfaces are not exactly spheroidal but are nearly spheroids with some bumps due to the inhomogeneities of the Earth's mass distribution. For mathematical simplicity, atmospheric and oceanic scientists approximate these geopotential coordinate surfaces geometrically as exact spheroids; that is, they use a coordinate system in which true gravity is exactly aligned with the vertical coordinate r and approximate the shapes of the iso-surfaces of r as spheroids. For clarity, we will henceforth refer to this approximation as the spheroidal geopotential approximation.

Line 9-13 in the Second Paragraph in CWSM23

However, as noted by CW22 and SM22,this analysis only quantifies the error introduced by making the absolute spheroidal approximation; that is, neglecting the horizontal

747 component of gravity in an absolute spheroidal coordinate system. It does not quantify the error in the community-standard spheroidal geopotential approximation described in the preceding paragraph; that is, in adopting geopotential coordinates and then approximating the shapes of the geopotentials as spheroids.

748

749 ***A9. Mistakenly treat the global mean sea level as the mean sea level.***

750 Chang (see Appendix B) uses a statement from the NOAA National Ocean Service
751 (https://oceanservice.noaa.gov/facts/geoid.html#:~:text=The%20geoid%20is%20a%20model,to%20measure%20precise%20surface%20elevations) that "the geoid is a model of
753 global mean sea level that is used to measure precise surface elevations" to mistakenly treat
754 the mean sea level (MSL) as the geoid. The NOAA National Geodetic Survey defines the
755 geoid as "The equipotential surface of the Earth's gravity field which best fits, in a least
756 squares sense, global MSL https://geodesy.noaa.gov/GEOID/geoid_def.html)".

757

[see **(E) in Subsection B2 of Appendix B] →

Note that NOAA ocean service also computes surface elevations based on the MSL geoid

758 (e.g. https://oceanservice.noaa.gov/facts/geoid.html#:~:text=The%20geoid%20is%20a%20model,to%20measure%20precise%20surface%20elevations.)

which shows that ellipsoidal height is not the only way to compute elevations.

759 Both National Ocean Service and National Geodetic Survey clearly show the connection of
760 the geoid to the global MSL but NOT to the MSL. The global MSL is the average MSL of
761 the entire ocean, i.e., a constant with no horizontal variation. However, the MSL has

762 horizontal variation. There are many spheroidal and true geopotential surfaces (see Section
763 2). The global MSL (a constant) is used to select the geoid from the set of true-geopotential
764 surfaces and to select the Earth spheroid surface (i.e., z = 0) from the set of spheroidal-
765 geopotential surfaces (see Figure 3). Considering such a confusion, the terminologies "MSL
766 geoid" and "MSL ellipsoid" created by Chang are wrong.

767 ***A10. Atmospheric and oceanic models and analyses are not formulated on the true***
768 ***geopotential coordinate system.***
769
770 CW22 and CWSM23 mistakenly treat the MSL as the geoid. The solid curve in Figure
771 B1 is the geoid surface rather than MSL. The coordinate system mentioned in CW22,
772 SM22, CWSM23, and Appendix B with MSL is NOT the true geopotential coordinate.
773

[see **(D) and (F) in Subsection B1 of Appendix B] →
On the MSL (a geoid), the horizontal component of gravity vanishes, hence the horizontal static pressure gradient force that balances it also vanishes, and they continue to vanish on upper level "constant height" surfaces as long as the heights are computed with respect to the MSL surface (a geoid) rather than a hypothetical ellipsoid as assumed by the author in Fig. 4. This confirms that, in practice, atmospheric and oceanic models and analyses are formulated on a geopotential (or geoid) coordinate system rather than an exact spheroidal coordinate system, and why atmospheric (and oceanic) analyses are close to geostrophically balanced despite not considering the horizontal components of gravity.

774

775

[see **(G) in Subsection B1 of Appendix B] →
However, as we emphasized in CW22 and CWSM23, the exact ellipsoid is not the coordinate system of choice in traditional GFD analyses or modeling. Instead, as stated in Gill (1982, which we cited in CW22 and quoted in CWSM23), atmospheric and oceanic scientists use the "true geopotential" (or geoid) surface (the solid curve in the figure above) (i.e., Fig. B1) as coordinate surfaces. These surfaces are perpendicular to ∇V, and thus gravity is exactly vertical in such a coordinate system, and there are no horizontal components of gravity in this (true) geopotential coordinate system.

776

777

[see **(H) in Subsection B1 of Appendix B] →
However, the main point of our comment was that the geophysical fluid dynamics community traditionally uses the "true geopotential surfaces" as coordinate surfaces to derive the component equations, and in such a coordinate system, gravity is exactly vertical, and I don't think the author really provided any concrete response in his analyses or argument to demonstrate that our comments were erroneous except in basically saying that we couldn't use such a coordinate system.

778

The wrong statement is caused by confusing the geoid with MSL. The geoid surface is a particular true geopotential surface, which best fits, in the least squares sense, the global MSL and represents the true horizontal surface. In the true geopotential coordinates, the geoid surface pressure would mean the pressure evaluated at about 106 m below the Earth reference spheroid in some locations such as to the south of India, and in other places close to 85 m above the Earth reference spheroid (Iceland) (Figure 7). No atmospheric and oceanic analytical or numerical model uses the true geopotential coordinate system. The "true geopotential surface" described in CW22, SM22, CWSM23, and Appendix B is NOT the true geopotential surface. The statement in the next box "the surface elevation of the lower boundary (which is the actual sea surface or air/sea interface) over oceans is always defined as 0 m. It confirms that the model that the authors of CW22, SM22, CWSM23 use is the exact spheroidal or exact spherical coordinates, i.e., does not even include fluctuation of the surface elevation (rigid boundary).

[see **(I) in Subsection B2 of Appendix B] →
If you refer to the surface elevation files from atmospheric and climate models, the surface elevation of the lower boundary (which is the actual sea surface or air/sea interface) over oceans is always defined as 0 m, which clearly indicates that the elevation used in atmospheric models refers to orthometric height (height referenced to the MSL geoid) rather than ellipsoidal height
(height referenced to the MSL ellipsoid, which is what Chu alleged to)

***A11. The MSL surface is not any type of geopotential surface.***

The authors of CW22, SM22, CWSM23 mistakenly treat the MSL as a true geopotential surface. Any geopotential surface should be *solely* determined by gravity such as spheroidal geopotential surface by the effective gravity $\mathbf{g}_e$, and geoid surface (with horizontal variation from 85 m to -106 m) by the true gravity $\mathbf{g}_t$. However, the MSL is under the influence of other forces such as winds, tides, and Coriolis force in addition to gravity. Thus, the MSL is not a geopotential surface of any type.

***A12. Confuse physical surface with its representation in coordinate systems.***

The sea level is an observable physical surface and can be represented by various coordinate systems with different values noted as the sea surface height. In meteorology and oceanography, the sea surface height is always referenced to the spheroidal-geopotential coordinates ($h_e$) such as in measurement by satellite altimetry https://ggos.org/item/satellite-altimetry/. However, the sea level can also be represented in the true-geopotential coordinates ($h_t$), $z_t = z_e - N$, with $N$ the geoidal undulation relative to the Earth reference ellipsoid [see Eq (18)]. Table 1 shows different representations of sea surface height, MSL, and global MSL in spheroidal and true geopotential coordinates.

No matter using, $h_e$ or $h_t$, MSL is the SAME surface. The mean sea level pressure (MSLP) is evaluated at MSL no matter using the spheroidal or true geopotential coordinates. This is to say that the MSLP is independent of the coordinate systems and always computed at MSL, and not at the geoid and the ellipsoid. MSLP is evaluated or computed on $z_e = S(\lambda, \varphi)$ in the spheroidal geopotential coordinates, and on $z_t = S(\lambda, \varphi) - N(\lambda, \varphi)$ in the true-geopotential coordinates. MSLP is NEVER computed on the ellipsoidal or geoidal surface. This statement is also valid for any pressure surface. Thus, the comments in the next three boxes in Appendix B are wrong.

[see **(J) in Subsection B2 of Appendix B] →
Chu argued that MSLP (and thus heights) in atmospheric science is computed with reference to the MSL ellipsoid, rather than the MSL geoid. This cannot be the case, since if this is true, MSLP over oceans will have to be computed not at the actual sea surface, but on the ellipsoid, which can be up to 100 m above or below the actual sea surface, since the actual sea surface is within 1-2 m of the MSL geoid (see, e.g., Maximenko et al. 2009)."

[see **(K) in Subsection B1 of Appendix B] →
If the author can persuade the WMO to change the definition of "surface" pressure from MSL pressure (pressure evaluated on the MSL surface which is a geoid where there is no horizontal gravity) to pressure computed on the reference spheroid
(not a constant geopotential surface where there is horizontal gravity), and compute geopotential height as height from the reference spheroid rather than height above MSL, then the author's equations containing horizontal gravity will have to be used to analyze geophysical data.

[see **(L) in Subsection B1 of Appendix B] →
Part of the confusion probably relates to the interpretation of how geopotential height is computed (Fig. 4 in this reply). In the author's derivation, the height of a pressure surface is computed with respect to a reference ellipsoid, hence there are height deviations related to the deviation of the geoid from the reference ellipsoid which contributes to the pressure gradient force that balances the horizontal gravity.

***A13. Confuse observable with non-observable surfaces.***

The MSL, ellipsoid, and geoid are three different surfaces. Among them, the MSL is observable physical surface and measured by tidal gauge or satellite altimeter. However, the ellipsoidal and geoidal surfaces (i.e., spheroidal and true geopotential surfaces) are non-observable and inferred by gravity field model (see Section 5). MSL is totally different from the ellipsoidal and geoidal surfaces. The terminologies "MSL geoid" and the "MSL ellipsoid"

created by Chang in Appendix B are wrong and have never been defined in meteorology, oceanography, and geodesy.

> [see **(J) in Subsection B2 of Appendix B] →
> Chu argued that MSLP (and thus heights) in atmospheric science is computed with reference to the MSL ellipsoid, rather than the MSL geoid. ...

***A14. Confuse fluid dynamics in rotating frame with in non-rotating frame.***

The authors of CW22, SM22, and CWSM23 confuse the fluid dynamics in rotating with non-rotating frame and mistakenly claim the static horizontal pressure gradient force largely cancels the horizontal component of the true gravity.

> Last paragraph in CWSM23
> Physically, as pointed out by CW22 and SM22, the reason why the horizontal components of gravity in a spheroidal (or spherical) coordinate system are not dynamically relevant is that in a fluid, static forces are largely balanced by a static pressure gradient force. The presence of horizontal gravity in the equations of motion will drive a static horizontal pressure gradient force that largely cancels this component of gravity.

> Last Paragraph in CWSM23
> Failure to account for this cancelation is also the fundamental flaw of Chu (2021), in which the author assumed that the horizontal components of gravity will drive Ekman transport instead of being largely balanced by a static horizontal pressure gradient force in spheroidal coordinates (see equations 17–20 of Chu 2021).

Anyone with basic knowledge of fluid dynamics and geophysical fluid dynamics knows that static forces are largely balanced by a static pressure gradient force only in nonrotating frame, not in rotating frame. Due to the Earth rotation, the steady-state dynamics under low Rossby number is the balance among the gravity, the pressure gradient force, and the Coriolis force, i.e., Eq (B1) in Appendix B with D**U**/D$t$ = 0, **F** = 0,

$$\rho_0\left(2\boldsymbol{\Omega}\times\mathbf{U}\right) = -\nabla p + \rho\nabla V \qquad \text{(A3)}$$

where $V$ is the true geopotential as in CWSM23. From the statement in Appendix B (see next box),

> [see **(M) in Subsection B1 of Appendix B] →
> Note that, conceptually, equation (B1) can be evaluated using a vector Lagrangian approach independent of any coordinate systems, and then the force balance based on the vector equation can subsequently be viewed on any "horizontal" surface by projecting all the vectors onto that surface. Thus, the physics (e.g. geostrophic balance) does not really involve any coordinate system.

We may project (A3) on the Earth spheroidal surface, which shows the balance among the Coriolis force, the horizontal components of the true gravity (i.e., horizontal gravity disturbance vector), and the horizontal pressure gradient force. Since the climatological datasets (or called static datasets) for the horizontal component of the true gravity, horizontal pressure gradient force, and the Coriolis force are all available online, the best way is to use these data rather than to use vague scale analysis to identify if the static horizontal pressure gradient force largely cancels the horizontal component of the true gravity or not. The D number [Eq (45) and Figure 12] clearly shows that *the static horizontal pressure gradient force does not cancel the horizontal component of the true gravity*.

***A15. Mistakenly decompose the gravity into gravitational and centrifugal accelerations.***

As mentioned in Introduction (Section 1), the ultimate cause to use gravity in oceanic and atmospheric dynamics is to make the centrifugal acceleration vanish in the equation of motion. However, the centrifugal force was stated explicitly in CW22 Supplementary, and implicitly in CWSM23 as the "neglected horizontal" component of $\mathbf{g}_e$. The "neglected horizontal" component of $\mathbf{g}_e$ in an exact spherical coordinate system is the centrifugal acceleration.

CW22 Supplementary

Note that while the horizontal component of the centrifugal force is stronger than the "horizontal" component of gravity associated with the wiggles in the true geopotential surfaces, the scale over which the centrifugal force varies is larger, hence the error associated with ignoring its variations can be smaller.

Line 10-12 in the Third Paragraphy in CWSM23

If we proceeded with Chu23's analysis and compared the magnitude of the "neglected horizontal"component of $\mathbf{g}_{eff}$ in an exact spherical coordinate system to the Coriolis force (equivalent to the C number of Chu23),we would find that C > 10.

Lines 13-16 in the Third Paragraph in CWMS23

On the contrary, this apparent paradox is resolved in the community-standard treatment of the spherical geopotential approximation (see Staniforth 2022) by redefining the vertical direction to be opposite $\mathbf{g}_{eff}$, such that the horizontal component of $\mathbf{g}_{eff}$ becomes exactly zero. The approximation then becomes an approximation of the geometry (i.e., approximating spheroids as spheres) rather than the neglect of the horizontal component of $\mathbf{g}_{eff}$, resulting in errors that are small (e.g., Bénard).

CW22 and CWSM23 intended to split $\mathbf{g}_e$ into gravitational acceleration and centrifugal acceleration. Such intention is equivalent to destroying the foundation of the atmospheric and oceanic dynamics.

***A16. Mistakenly treat the Earth mass density as the Earth surface mass distribution.***

The mass density $\sigma(\mathbf{r})$ represents mass distribution inside the Earth and related to the internal structure of the Earth such as crust, mantle, inner core, and outer core. *It is not the Earth surface mass distribution from spherical to near spheroid.* The Earth gravitational acceleration is the volume integration over the whole solid Earth with $\sigma(\mathbf{r})$ as part of the integrand [see Eq (1)].

> First Paragraph in CWSM23
> The rotation of the Earth produces a centrifugal force which distorts the Earth's mass distribution from spherical to nearly spheroidal with small spatial inhomogeneities...
> ...If Earth's mass distribution were exactly spheroidal, the geopotential would also be exactly spheroidal, and net gravity due to this hypothetical geopotential would be perpendicular to spheroidal surfaces—this is the $\mathbf{g}_{eff}$ defined by Chu (2023; hereafter Chu23). However, the Earth's mass distribution is not exactly spheroidal, and the (slightly) uneven mass distribution gives rise to a perturbation field $\delta\mathbf{g}$. The true (or total) gravity $\mathbf{g}$ is the sum of $\mathbf{g}_{eff}$ and $\delta\mathbf{g}$.

***A17. Confuse the differences between ($\Phi_t$ to $\Phi_e$) and between ($\Phi e$ to $\Phi_s$).***

CWMS23 stated the difference from using the spheroidal geopotential ($\Phi_e$) to using the spherical geopotential ($\Phi_s$):

> Lines 3 – 6 in Third Paragraph in CWMS23
> This is analogous to the spheroidal geopotential approximation described above: the vertical coordinate is aligned with geopotentials, and then those geopotentials are approximated as spheres instead of spheroids. This approximation is also adopted by Chu23, stating that the errors of such an approximation are small (last paragraph in section 2.2 of Chu23).

But questioned about the difference from using the true geopotential ($\Phi_t$) coordinates to spheroidal geopotential ($\Phi_e$) coordinates:

> Lines 6 – 9 in Third Paragraph in CWMS23
> It is inconsistent of Chu23 to apply this spherical geopotential approximation while insisting that the spheroidal geopotential approximation cannot be applied to the smaller variations in the geopotential field due to the Earth's uneven mass distribution.

Section 3 and Table 2 show that the difference from ($\Phi_e$) to ($\Phi_s$) is negligible, and the difference from ($\Phi_t$) to ($\Phi_e$) is non-negligible.

***A18. Mistakenly treat the sea surface elevation referenced to the geoid not to the ellipsoid.***

In oceanography and meteorology, the sea surface elevation (i.e., sea surface height) is always referenced to the spheroidal geopotential coordinates ($h_e$) such as in measurement by satellite altimetry https://ggos.org/item/satellite-altimetry/. Chang's comment below is wrong.

> [see **(I) in Subsection B2 of Appendix B] →
> If you refer to the surface elevation files from atmospheric and climate models, the surface elevation of the lower boundary (which is the actual sea surface or air/sea interface) over oceans is always defined as 0 m, which clearly indicates that the elevation used in atmospheric models refers to orthometric height (height referenced to the MSL geoid) rather than ellipsoidal height (height referenced to the MSL ellipsoid, which is what Chu alleged to)

***A19. Mistakenly use reanalysis by model excluding $g_0\nabla N$ to deny the importance of $g_0\nabla N$.***

NCEP reanalyzed long term January mean sea level pressure (MSLP) in Subsection B3 of Appendix B is used by Chang to deny the importance of the horizontal gravity disturbance vector $g_0\nabla N$. The NCEP reanalysis is produced by the NCEP Global Forecast System (GFS), which excludes the horizontal gravity disturbance vector $g_0\nabla N$. To use a system without $g_0\nabla N$ to deny the importance of $g_0\nabla N$ is wrong.

***A20. The ultimate statement in CWSM23 is wrong.***

Section 3 and Table 2 clearly show that the spheroidal geopotential surface approximation proposed by the authors of CW22, SM22, CWSM23 has an evident horizontal pressure gradient error due to the difference between the spheroidal and true geopotential coordinates. The error is the same as the horizontal component of the true gravity ($g_0\nabla N$). The statement in the next box is wrong.

> From Abstract in CWSM23
> In recent papers by the authors [Chang and Wolfe (2022; CW22) and Stewart and McWilliams (2022; CW22)], we explained that the actual interpretation of the approximation made in atmospheric and oceanic modeling is not neglecting the horizontal component of the true gravity, but is a geometrical approximation, approximating nearly spheroidal geopotential surfaces with bumps on which the true gravity is vertical by exactly spheroidal surfaces.

## Appendix B. Additional comments by Chang on Chu (21a, b, c) and Chu (2023) to DAO

### *B1. Dr. Chang's comments sent to DAO on 21 August 2023*

Since the author's "reply" is directed to a comment that I was the lead author of, I think it should be more appropriate for me to sign my review. - Edmund Chang.

I think most of the derivations in this rather lengthy "short communication" are fine but irrelevant as a reply. Overall, I don't think the author responded to the main point of the comment by CW22 and CWSM23. In these comments, we completely agreed with the author that in an exact spheroidal coordinate system as that used by the author in his derivations, gravity is not vertical, and so there are horizontal components of gravity that are not negligible. Much of the derivation in this reply basically reinforces this point which we did not question. **(H) However, the main point of our comment was that the geophysical fluid dynamics community traditionally uses the true geopotential surfaces as coordinate surfaces to derive the component equations, and in such a coordinate system, gravity is exactly vertical, and I don't think the author really provided any concrete response in his analyses or argument to demonstrate that our comments were erroneous except in basically saying that we couldn't use such a coordinate system. Another key point we made was that in a coordinate system in which gravity is not vertical, the horizontal components of gravity are largely balanced by a static pressure gradient force. The author attempted to dispute that, but as I will show later, the author's claim can be shown to be erroneous. Thus, in my opinion, this reply completely fails to refute our criticism of the author's papers.

Let me elaborate a bit more (while trying not to repeat everything contained in CW22 and CWSM23), making use of some of the figures that the author used as illustrations. As we discussed in CW22, mathematically, the vector equation is independent of the coordinate system:

$$\rho_0\left[\frac{D\mathbf{U}}{Dt}+2\boldsymbol{\Omega}\times\mathbf{U}\right]=-\nabla p+\rho\nabla V+\rho_0\mathbf{F} \tag{B1}$$

In (B1), $V$ is the true geopotential, including the effect of earth's gravitational pull and centrifugal force due to rotation, and surfaces of constant $V$ are near spheroidal but with bumps, much like Fig. 3 of the author's note (except that the deviations of the geoid from the ellipsoid are greatly exaggerated in the figure), which is reproduced below:

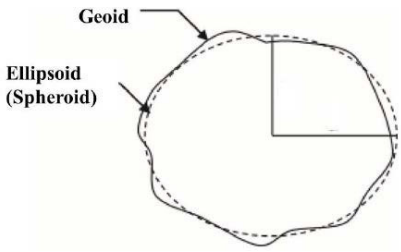


**Figure B1**. Geoid and ellipsoid.

**(M) Note that, conceptually, equation (B1) can be evaluated using a vector Lagrangian approach independent of any coordinate systems, and then the force balance based on the vector equation can subsequently be viewed on any "horizontal" surface by projecting all the vectors onto that surface. Thus, the physics (e.g. geostrophic balance) does not really involve any coordinate system. Nevertheless, to facilitate discussion and for ease of numerical computation, a coordinate system is usually adopted.

As the author wrote, the true geopotential surface is the geoid surface (the solid curve in the figure above). To express (1) in component form (e.g. to facilitate modeling), one has to pick a coordinate system. The author picked the ellipsoid (or spheroid, or the dashed curve in the figure) to coincide with a coordinate surface, and on that surface, gravity is not perpendicular to the coordinate surface and thus has horizontal components, and the author estimated that the magnitude of the ratio between the horizontal component of gravity (which is a *static* force) and the Coriolis force (the author's $C$ number) is of order slightly less than 1, hence not negligible. In this analysis, the author implied that the magnitude of the *dynamical* errors can be represented by the $C$ number (the author's equation 37 in the reply).

**(G) However, as we emphasized in CW22 and CWSM23, the exact ellipsoid is not the coordinate system of choice in traditional GFD analyses or modeling. Instead, as stated in Gill (1982, which we cited in CW22 and quoted in CWSM23), atmospheric and oceanic scientists use the true geopotential (or geoid) surface (the solid curve in the figure above) as coordinate surfaces. These surfaces are perpendicular to $\nabla V$, and thus *gravity is exactly vertical in such a coordinate system, and there are no horizontal components of gravity in this (true) geopotential coordinate system*. **(A) So, what kind of approximation is needed for using this coordinate system? If we examine (1) carefully, all terms in the equation are local, except for the acceleration term, which involves how the coordinate axes change as a function of space. As CW22 pointed out, in component form, the acceleration term can be written as:

$$\frac{D\mathbf{U}}{Dt} = \mathbf{i}\frac{Du}{Dt} + \mathbf{j}\frac{Dv}{Dt} + \mathbf{k}\frac{Dw}{Dt} + u\frac{D\mathbf{i}}{Dt} + v\frac{D\mathbf{j}}{Dt} + w\frac{D\mathbf{k}}{Dt} \qquad \text{(B2)}$$

The last 3 terms in equation (B2) are the metric terms. Given the local directions of the 3 coordinate axes (which are well defined once we know the coordinate surfaces) and how they change in space, all terms in (B1) can be exactly evaluated at any location. However, it is mathematically extremely challenging to evaluate the metric terms in (B2) exactly in the irregular geopotential coordinate system. The approximation made in GFD is to calculate the metric terms in (B2) using the metric terms for a spheroid (or a sphere for the spherical geopotential approximation). That is why CW22 stated that the errors are in the metric terms (which CW22 estimated to be small), not in the neglect of the horizontal gravity. The author insisted that the errors are not only in the metric terms but also in the neglect of horizontal gravity because he insisted on formulating his component equations on the exact spheroid ($z_e$ in the reply) rather than on the true geopotential surfaces ($z_t$ in his reply). In fact, I think he did agree that there are no horizontal components of gravity on the true geopotential surfaces (p. 10). **(A) Note that, as will be discussed below, for the irregular geopotential coordinate, other than the pressure gradient force and gravity, the

horizontal components of the other 3 terms in equation (B1) can be evaluated on a spheroid that passes through the same point with only minor errors (relative error of the order of magnitude of the angle between the true geopotential surfaces and a spheroid, which is of the order $10^{-4}$ as estimated by CW22).

The recent textbook by Staniforth (2022, cited by CWSM23) provided a nice discussion on why the component equations should be expressed on geopotential coordinates (section 7.3), and the ideas are very similar to those described in CW22 (we did not know about that book until after we published CW22). Basically, if one uses a coordinate system that does not coincide with the geopotential surfaces, gravity is not vertical in that system, hence there will be horizontal components of gravity (just like in the equations derived by the author), and traditional force balances (such as geostrophic balance) will appear to be more complicated because it will involve the horizontal components of gravity, which is basically what the author's papers have been about. As we pointed out in CW22 and CWSM23 (and by Staniforth 2022), in such a coordinate system, horizontal gravity will force a static horizontal pressure gradient force to largely balance that. In such a coordinate system, the part of the horizontal pressure gradient force that balances the Coriolis force will then appear as a deviation from the static pressure gradient force. This horizontal gravity and the static horizontal component of the pressure gradient force that balances it are absorbed into the vertical force balance when a true geopotential coordinate system is used. The physics hasn't really changed, but the interpretation in the geopotential coordinate system is much simpler.

**(B) The author argued that this is not the case, i.e., static gravity will not be balanced by a static pressure gradient force alone but also by a "static Coriolis force" (p. 18). Let us consider why that cannot be the case. Consider equation (B1). The "force balance" consisting of all terms in (B1) must be valid regardless of the coordinate system. Let us first examine horizontal force balance on a constant true geopotential surface. On such a surface, the horizontal component of gravity is exactly zero. Hence the other terms must be exactly balanced. Scale analysis suggests that Coriolis force balances the horizontal pressure gradient force on this surface (or geostrophic balance), but this is actually not crucial. Now let us examine the force balance on a surface that is slightly tilted with respect to the true geopotential surface (e.g., an exactly spheroidal surface) that passes through the same point in space. On this surface, the horizontal components of all the vectors in (B1) are different from those on the constant geopotential surface. However, if we consider a vector that has both horizontal and vertical components on the constant geopotential surface, with magnitude $v_h$ and $v_v$ respectively, a slight tilt of the horizontal surface by an angle $\alpha$ produces a change in the magnitude of the horizontal component at most by $v_h$ (1-cos $\alpha$), or order $v_h\alpha^2$ for a small angle $\alpha$, while tilting the vertical component can produce a change in the horizontal component by $v_v \sin\alpha$, or $v_v\alpha$ for small angle $\alpha$. Consider the terms in (B1), the Coriolis force, friction, and acceleration terms all have vertical components that are at most of the same order of magnitude as their horizontal components (or smaller), and hence tilting the coordinate surface by a small angle $\alpha$ can at most change the horizontal magnitude of these forces by a fraction of the order of $\alpha$ of its original horizontal magnitude. On the other hand, the vertical components of gravity and the pressure gradient force are

much stronger than their horizontal components, hence tilting the horizontal surface by an angle α will change the magnitude of the horizontal component of these two forces by the order of magnitude of their *vertical* component times α, which is much larger than their horizontal component times α, and much larger than the change in horizontal components of all the other terms in (A1). This analysis clearly shows that force balance viewed on surfaces that are tilted slightly from constant geopotential surfaces (e.g., exactly spheroidal surfaces) must have the new horizontal components of gravity largely balanced by a new static horizontal pressure gradient force, and not by a new static horizontal Coriolis force since the horizontal Coriolis force observed on such a surface can only differ slightly (by a fractional difference of order α) from that observed on a constant geopotential surface. Note that as pointed out by CW22, the angle α between a true geopotential surface and the reference spheroid is of the order $10^{-4}$ radians.

Since this is a key point, let us examine this further from a slightly different (but related) angle. As observed on a constant geopotential surface (where there is no horizontal gravity), for large scale atmospheric and oceanic motions, the vertical balance (perpendicular from the surface) must be between the static force of vertical gravity and the oppositely directed static vertical pressure gradient force. Viewed from a slightly tilted surface (e.g., a spheroid passing through the same point), the vertical gravity perpendicular to the geopotential surface projects onto this slightly tilted spheroidal surface to give rise to a horizontal gravity perturbation vector. At the same time, the oppositely directed vertical static pressure gradient force perpendicular to the geopotential surface must also project onto the spheroidal surface to give rise to a static horizontal pressure gradient that is equal and opposite to the static horizontal gravity. This must be true as long as the vertical force balance is largely hydrostatic.

**(L) Part of the confusion probably relates to the interpretation of how geopotential height is computed (Fig. 4 in this reply). In the author's derivation, the height of a pressure surface is computed with respect to a reference ellipsoid, hence there are height deviations related to the deviation of the geoid from the reference ellipsoid which contributes to the pressure gradient force that balances the horizontal gravity. **(C) However, in atmospheric and oceanic sciences, geopotential heights are computed with reference to the mean sea level (MSL), which is very close to a geoid but deviates from a reference ellipsoid. The MSL pressure (pressure on the hypothetical mean sea level which should coincide with a geoid if the ocean is motionless) is first computed, and then the thickness is added to find the height of pressure surfaces above (or below) MSL, which practically is the distance of the upper level (or below sea-level) pressure surfaces from the mean sea level geoid. Hence the way that the geopotential heights are computed in practice means that the values are the height with respect to a reference geoid (the MSL) rather than the height with respect to a reference ellipsoid. **(D) On the MSL (a geoid), the horizontal component of gravity vanishes, hence the horizontal static pressure gradient force that balances it also vanishes, and they continue to vanish on upper level "constant height" surfaces as long as the heights are computed with respect to the MSL surface (a geoid) rather than a hypothetical ellipsoid as assumed by the author in Fig. 4. **(F) This confirms that, in practice, atmospheric and oceanic models and analyses are formulated on a geopotential (or geoid) coordinate system

rather than an exact spheroidal coordinate system, and why atmospheric (and oceanic) analyses are close to geostrophically balanced despite not considering the horizontal components of gravity. **(K) If the author can persuade the WMO to change the definition of "surface" pressure from MSL pressure (pressure evaluated on the MSL surface which is a geoid where there is no horizontal gravity) to pressure computed on the reference spheroid (not a constant geopotential surface where there is horizontal gravity), and compute geopotential height as height from the reference spheroid rather than height above MSL, then the author's equations containing horizontal gravity will have to be used to analyze geophysical data. But in that case, "surface" pressure would mean the pressure evaluated at about 100 m above the actual sea surface in some locations such as to the south of India, and in other places close to 100 m below the sea surface (e.g. equatorial Western Pacific and western Atlantic off the UK; see Fig. 1 of Chu's retracted paper published in Scientific Reports). Note that this is a point that we also briefly mentioned in CW22, although not with this amount of details.

Finally, note that in CWSM23 we did not claim that the analyses of Chu23 were wrong. We just noted that the results of that paper were irrelevant to the dynamical balances, since the author did not consider the possibility that the horizontal components of gravity (in his coordinate systems) are largely balanced by a static horizontal pressure gradient force. On the other hand, as pointed out by CWSM23, the analyses of Chu (2021) were erroneous, because in that paper the author ignored this static pressure gradient force, and erroneously assumed that horizontal gravity will drive a much stronger.

***B2. Dr. Chang's comments sent to DAO on 29 August 2023***

In this revised reply, **(J) Chu argued that MSLP (and thus heights) in atmospheric science is computed with reference to the MSL ellipsoid, rather than the MSL geoid. This cannot be the case, since if this is true, MSLP over oceans will have to be computed not at the actual sea surface, but on the ellipsoid, which can be up to 100 m above or below the actual sea surface, since the actual sea surface is within 1-2 m of the MSL geoid (see, e.g., Maximenko et al. 2009, *JTECH*). Over the ocean, in atmospheric science, the common practice in atmospheric analysis and modeling is to define the surface pressure as the MSLP. **(I) If you refer to the surface elevation files from atmospheric and climate models, the surface elevation of the lower boundary (which is the actual sea surface or air/sea interface) over oceans is always defined as 0 m, which clearly indicates that the elevation used in atmospheric models refers to orthometric height (height referenced to the MSL geoid) rather than ellipsoidal height (height referenced to the MSL ellipsoid, which is what Chu alleged to). Hence the entire revised reply is based on an erroneous assumption. **(E) Note that NOAA ocean service also computes surface elevations based on the MSL geoid (e.g. https://oceanservice.noaa.gov/facts/geoid.html#:~:text=The%20geoid%20is%20a%20model,to%20measure%20precise%20surface%20elevations.) which shows that ellipsoidal height is not the only way to compute elevations.

***B3. Dr. Chang's comments sent to DAO on 30 August 2023***

One additional point. If indeed MSLP is computed on the MSL spheroid (or ellipsoid), given that the geopotential has significant undulations on the spheroid, as shown in Fig. 1 of Chu's original retracted paper in Scientific Reports, which I have reproduced below:

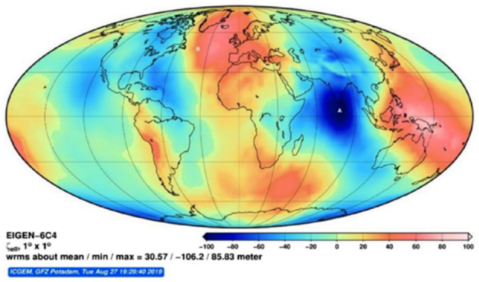


Figure 1. Digital data for EIGEN-6C4 geoid undulation (*N*) with 1°×1°, computed online at the website http://icgem.gfz-potsdam.de/home.

**Figure B2.** Digital data for EIGEN-6C4 geoid undulation (N).

At the equator, to the south of the southern tip of India, there is a depression of about -100 m, while over New Guinea, there is a high of about +80 m. This means that there is strong "horizontal" gravity between these two points on the spheroid. This geopotential height difference corresponds to a pressure difference of about 24 hPa (dp = -rho*g*dh). Hence if we apply Chu's equations, if MSLP is indeed computed on the spheroid and not on the geoid, there must be a pressure difference of about 24 hPa to balance that geopotential difference. However, it is well known that pressure gradients are weak in the tropics, and indeed, if one plots the climatological pressure (MSLP) distribution, e.g. for January, there is very little pressure difference between these two points:

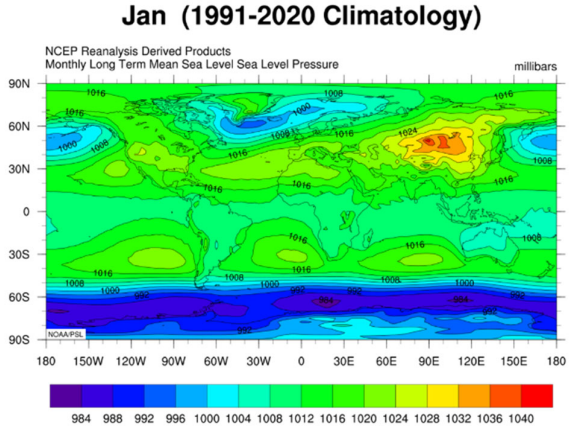


**Figure B3**. NCEP reanalyzed long term January mean sea level pressure (MSLP).

The figure above shows that there is very little pressure difference between the aforementioned points at the equator, which clearly demonstrates that MSLP is computed on the MSL geoid, where there is no horizontal gravity between these two points and hence no horizontal pressure gradient is needed to balance that.

## References


Beńard, P. (2015). An assessment of global forecast errors due to the spherical geopotential approximation in the shallow-water case. *Quarterly Journal of Royal Meteorological Society*, **141**, 195-206.

Chang, E.K.M., & Wolfe, C.L.P. (2022). The "horizontal" components of the real gravity are not relevant to ocean dynamics. *Scientific Reports, Matters Arising* https://www.nature.com/articles/s41598-022-09967-3.

Chang, E.K.M., Wolfe, C.L.P., Stewart, A.L. & McWilliams, J.C. (2023). Comments on "horizontal gravity disturbance vector in atmospheric dynamics" by Peter C Chu. *Dynamics of Atmospheres and Oceans*, **103**, 101382, https://www.sciencedirect.com/science/article/pii/S0377026523000337.

Chu, P. C. (2021a). Ocean dynamic equations with the real gravity. *Scientific Reports*, **11**, Article Number 3235, https://doi.org/10.1038/s41598-021-82882-1 (wrongly retracted by the Chief Editor).

Chu, P. C. (2021b). True gravity in atmospheric Ekman layer dynamics. *Journal of Geophysical Research*, **126**, e2021JD035293, https://doi.org/10.1029/2021JD035293 (wrongly retracted by then the Editor in Chief).

Chu, P. C. (2021c). True gravity in ocean dynamics Part-1 Ekman transport. *Dynamics of Atmospheres and Oceans*, **96**, 101268, https://doi.org/10.1016/j.dynatmoce.2021.101268.

Chu, P. C. (2023). Horizontal gravity disturbance vector in Atmospheric dynamics. *Dynamics of Atmospheres and Oceans,***102**, 101369, https://www.sciencedirect.com/science/article/pii/S0377026523000209.

Gates, W.L. (2004). Derivation of the equations of atmospheric motion in oblate spheroidal coordinates. *Journal of Atmospheric Sci*ences, **61**, 2478-2487.

Gill, A. E. (1982). *Atmosphere-Ocean Dynamics*. Academic Press (Page 46, Equation 3.5.2 for the effective gravity, and Page 92, Error less than 0.17% between polar spherical coordinate and oblate spheroidal coordinate systems).

Kessler, W. S. (1990). Observations of long Rossby waves in the northern tropical Pacific. *Journal of Geophysical Research*, **95**, 5183–5217.

Kostelecký, J., Klokočnìk, J., Bucha, B., Bezděk, A., & Förste, C. (2015). Evaluation of the gravity model EIGEN-6C4 in comparison with EGM2008 by means of various functions of the gravity potential and by BNSS/levelling. *Geoinformatics FCE CTU*, **14** (1), http://doi.org//10.14311/gi.14.1.1.

Munk, W.H. (1950). On the wind-driven ocean circulation. *Journal of Meteorology*, **7**, 79-93.

Pedlosky, J. (1987). *Geophysical Fluid Dynamics* (Second Edition), Springer, New York (see Pages 46-47 for the effective gravity $\mathbf{g}_e$, and Page 286 for the traditional combined Sverdrup-Stommel-Munk equation).

Sandwell, D.T., & Smith, W.H.F. (1997). Marine gravity anomaly from Geosat and ERS 1 satellite altimetry. *Journal of Geophysical Research*, **102**, B5, 10,039-10,054.

Staniforth, A., & White, A. (2015). Geophysically realistic, ellipsoidal, analytically tractable

(GREAT) coordinates for atmospheric and oceanic modeling. *Quarterly Journal of Royal Meteorological Society*, **141**, 1646-1657.

Stommel, H. (1948). The westward intensification of wind-driven ocean currents. *Transactions of American Geophysical Union*, **29** (2), 202-206.

Stewart, A.L., & McWilliams, J.C. (2022). Gravity is vertical in geophysical fluid dynamics. *Scientific Reports, Matters Arising*, https://www.nature.com/articles/s41598-022-10023-3.

Sverdrup, H. U. (1947). Wind-driver currents in a baroclinic ocean; with application to the equatorial current of the eastern Pacific, *Proceedings National Academy of. Sciences*, **33**, 318-326.

Vaníček, P., & Krakiwsky, E. (1986). *Geodesy: the Concepts*. North-Holland, Amsterdam, [see Equation (6.4) on Page 72].